

# Feedback Control of Traveling Wave Solutions of the Complex Ginzburg Landau Equation

K.A. Montgomery<sup>†</sup> and M. Silber<sup>†</sup>

<sup>†</sup> Department of Engineering Sciences and Applied Mathematics, Northwestern University, Evanston, IL 60208 USA

**Abstract.** Through a linear stability analysis, we investigate the effectiveness of a noninvasive feedback control scheme aimed at stabilizing traveling wave solutions  $Re^{iKx+i\omega t}$  of the one-dimensional complex Ginzburg Landau equation (CGLE) in the Benjamin-Feir unstable regime. The feedback control is a generalization of the time-delay method of Pyragas [1], which was proposed by Lu, Yu and Harrison [2] in the setting of nonlinear optics. It involves both spatial shifts, by the wavelength of the targeted traveling wave, and a time delay that coincides with the temporal period of the traveling wave. We derive a single necessary and sufficient stability criterion which determines whether a traveling wave is stable to all perturbation wavenumbers. This criterion has the benefit that it determines an optimal value for the time-delay feedback parameter. For various coefficients in the CGLE we use this algebraic stability criterion to numerically determine stable regions in the  $(K, \rho)$ -parameter plane, where  $\rho$  is the feedback parameter associated with the spatial translation. We find that the combination of the two feedbacks greatly enlarges the parameter regime where stabilization is possible, and that the stability regions take the form of stability tongues in the  $(K, \rho)$ -plane. We discuss possible resonance mechanisms that could account for the spacing with  $K$  of the stability tongues.

Submitted to: *Nonlinearity*

## 1. Introduction

A current challenge to our understanding of pattern-forming systems lies in our ability to control the spatio-temporal chaos that many of these systems naturally exhibit. The mathematical existence of a plethora of simple spatial or spatio-temporal patterns for many nonequilibrium, spatially extended systems is well-established on the basis of equivariant bifurcation theory [3]. However, these simple patterns often prove to be unstable in a given system, which evolves instead to a state of spatio-temporal chaos. Perhaps the simplest and best studied manifestation of spatio-temporal chaos is that associated with the one-dimensional complex Ginzburg Landau equation (CGLE) [4], a universal amplitude equation that describes spatially-extended systems in the vicinity of a Hopf bifurcation. In the so-called Benjamin-Feir unstable regime, the simple solutions (*e.g.* traveling plane waves and spatially-homogeneous oscillations) are all unstable to long-wave perturbations. The focus of this paper is a linear stability analysis of Benjamin-Feir unstable traveling wave solutions of the CGLE in the presence of a feedback control scheme that was originally proposed by Lu, Yu and Harrison [2] in the setting of nonlinear optics. The feedback approach is noninvasive, meaning that the feedback signal decays to zero once the targeted traveling wave state of the system is realized.

Feedback control methods aimed at stabilizing the unstable periodic orbits associated with low-dimensional chaotic attractors have been extensively investigated for more than ten years now, and have proved especially effective for nonlinear optical systems. The simple approach taken by Ott, Grebogi and Yorke [5] relies on applying small perturbations to a system parameter that help maintain the system in a neighborhood of the desired unstable periodic orbit. However, this approach, which requires an active monitoring of the state of the system so that the feedback is appropriately adjusted, can prove impractical in systems that evolve too rapidly. Autoadjusting feedback control methods, in which the feedback is based upon current and past states of a system, have proven useful for rapidly evolving systems because they adjust automatically to rapid changes of the system and require no active monitoring. One autoadjusting feedback technique that has attracted considerable attention was introduced by Pyragas [1]. In this approach the feedback is proportional to the difference between the current and past states of a system, *i.e.* the feedback is  $F = \gamma(x(t) - x(t - \Delta t))$ , where  $\Delta t$  is the period of the targeted unstable periodic orbit. The method possesses a couple of properties which make it attractive experimentally. First, if a state with the desired periodicity is stabilized the feedback term vanishes and control is achieved in a reasonably noninvasive manner. Second, this type of feedback control may be straightforward to implement in the laboratory when feedback loops are practical. The method has been implemented successfully in a variety of experimental systems including electronic [6, 7], laser [8], plasma [9, 10, 11], and chemical systems [12, 13, 14]. A number of modifications of the method of Pyragas have also been investigated. For instance, Labate *et al.* [15] added a filter to their time delayed feedback

scheme for a  $CO_2$  laser and successfully stabilized periodic behavior; the filter rejected one of the characteristic frequencies associated with a quasiperiodic route to chaos in this system. In yet another direction Socolar *et al.* [16] proposed a method of “extended time delay autosynchronization” which incorporates information about the state of the system at many earlier times  $t - n\Delta t$  (prescribed by positive integers  $n$ ). This extended time delay feedback can successfully stabilize traveling wave solutions of the one-dimensional CGLE [17], although it fails in two-dimensions [18].

For spatially extended pattern forming systems, modifications of the time-delay autosynchronization scheme of Pyragas have been proposed which take into account not only the temporal periodicity, but also the spatial periodicity of the targeted pattern. Perhaps the simplest such scheme is the one proposed in [2], which is the one we investigate here. Specifically, Lu, Yu and Harrison used numerical simulations of the two-dimensional Maxwell-Bloch equations describing a three level laser system to demonstrate that spatio-temporal chaos (“optical turbulence”) could be eliminated by applying a linear combination of time-delay feedback and an analogous feedback term involving a spatial translation, *i.e.*,  $F = \rho(E(\mathbf{x} + \mathbf{x}_0) - E(\mathbf{x}))$ , where  $\mathbf{x}_0$  is the translation vector associated with the feedback. Other schemes for controlling spatio-temporal patterns have incorporated spatial filters in the time-delayed feedback. For instance, Bleich *et al.* [19] showed, through linear stability calculations and numerical simulations, that traveling wave solutions of a model of a spatially extended semiconductor laser could be stabilized using a combination of a Fourier filter and an extended time-delay scheme involving multiple time delays. Baba *et al.* [20] considered problems for which a Fourier filter is not appropriate; they incorporate a spatio-temporal filter in their time-delay feedback that is derived from a linear stability analysis of the targeted unstable periodic orbit in the uncontrolled problem. Other successful approaches to feedback control of spatial patterns in nonlinear optics have relied on the Fourier filters alone [21, 22, 23, 24, 25]. Numerous investigations of oscillatory chemical patterns have incorporated a global time-delay feedback control [26, 27, 28, 29]. In this case the magnitude of the global feedback depends on the spatial average of a chemical concentration at an earlier time. Global delayed feedback has been shown to suppress spatio-temporal chaos associated with the CGLE [30, 31].

The goal of our paper is to provide a detailed analysis of the spatial and temporal feedback control scheme proposed by Lu, Yu, and Harrison [2]. In particular our goal is to derive conditions under which this method can stabilize traveling waves in the Benjamin-Feir unstable regime of the CGLE. The analysis is complicated because of the time-delay, and because we must determine stability with respect to perturbations at all spatial wavenumbers. On the other hand, it is simplified because the exact traveling wave solutions of the CGLE (both with and without feedback) take the particularly simple plane wave form  $Re^{iKx+i\omega t}$  (where  $R$  and  $\omega$  are simple functions of the wavenumber  $K$ ). Moreover, as is the case for the CGLE without feedback, the plane wave solution enters the linear stability analysis only parametrically through the wavenumber  $K$ . Specifically, the linear stability analysis reduces to an investigation

of a pair of complex linear delay-differential equations whose coefficients depend on the wavenumber  $K$  of the targeted plane wave solution and the wavenumber  $Q$  of the perturbation but not explicitly on the spatial variable  $x$  (nor on time). Our main linear stability result is an algebraic condition that determines whether or not there exists a time-delay feedback term that will stabilize the traveling wave (for a given spatially-shifted feedback term). Interestingly, our analysis identifies an *optimal* time delay feedback to use in determining whether the spatial and temporal feedback control method will stabilize the traveling wave. Our algebraic condition for stability, which must be checked numerically, reveals that the combination of temporal-delays and spatial-shifts in the feedback greatly enlarges the regions where stabilization is possible. In some instances we are able to understand the failure of the feedback control scheme in terms of simple resonant conditions between the wavenumber  $K$  of the underlying traveling wave pattern and the wavenumber  $Q$  of the unstable perturbation, or between the frequency  $\omega$  of the traveling wave and the frequency associated with the perturbation. These resonances can be tuned to some extent using the spatially-shifted feedback term and thus are not fundamental obstacles of the type that can be present when time-delay feedback alone is used [32, 33, 34]. (Another approach to eliminating fundamental limitations of time-delay feedback in low-dimensional chaotic systems has been proposed and investigated by Pyragas [35].) We expect our paper to contribute to the body of literature in which the success of time-delay feedback methods is investigated through a detailed linear stability analysis of the associated delay-differential equations [36, 37, 38, 32, 39].

Our paper is organized as follows. In section 2 we describe the feedback to be investigated, and review the basic properties of traveling wave solutions of the CGLE without feedback. This section also reviews the stability analysis of a related problem, in which a time delay feedback term was applied to a system near a Hopf bifurcation [40]. Section 3 sets up our linear stability analysis for the traveling wave solutions of the CGLE in the presence of feedback. We then prove our main stability result which allows us to determine the conditions under which the feedback parameters can be chosen so that Benjamin–Feir unstable traveling waves are stabilized. In section 4, we apply our stability criterion to numerically determine the parameter regions in which feedback control is possible, and discuss possible cause for failure. Finally, in section 5, we summarize our results and suggest possible extensions of our analysis.

## 2. Background and Problem Formulation

The 1-D complex Ginzburg Landau equation, an amplitude equation describing a spatially extended system near the onset of a Hopf bifurcation, is given by

$$\partial_t A = A + (1 + ib_1)\partial_x^2 A - (b_3 - i)|A|^2 A. \quad (1)$$

where  $A(x, t)$  is a complex amplitude, and  $b_1$  and  $b_3$  are real parameters. We consider traveling wave solutions of (1) of the form

$$A_{TW} = R e^{iKx + i\omega t}, \quad (2)$$

where the amplitude  $R$  and frequency  $\omega$  are determined by the wavenumber  $K$  through the relations

$$R^2 = \frac{(1 - K^2)}{b_3}, \quad (3)$$

$$\omega = R^2 - b_1 K^2. \quad (4)$$

We focus on the case of a supercritical Hopf bifurcation so that  $b_3 > 0$ ; thus  $|K| < 1$  follows from (3).

In the Benjamin–Feir unstable regime ( $b_1 > b_3 > 0$ ), all plane wave solutions of the form (2) are unstable. In the Benjamin–Feir stable regime ( $b_1 < b_3$ ,  $b_3 > 0$ ), traveling waves with wavenumbers  $K$  satisfying  $0 \leq K^2 < K_{max}^2 = (b_3 - b_1)/(3b_3 - b_1 + 2/b_3)$  are linearly stable to longwave perturbations [41, 42, 43]. Figure 1 summarizes the behavior of typical solutions of (1) in the  $(b_1, b_3)$ -parameter plane. The Benjamin–Feir unstable regime is divided into three different regions, an amplitude turbulent regime, a phase turbulent regime, and a bichaotic regime. The amplitude turbulent regime is characterized by large fluctuations in amplitude and phase defects. In the phase turbulent regime amplitude fluctuations are much smaller and no defects are observed. In the bichaotic regime either amplitude or phase turbulence occurs depending upon initial conditions [4].

We consider how feedback of the type proposed in [2] affects the linear stability of the plane wave solutions of the CGLE in the Benjamin–Feir unstable regime. In particular, we consider

$$\partial_t A = A + (1 + ib_1) \partial_x^2 A - (b_3 - i) |A|^2 A + F \quad (5)$$

where the feedback term,  $F$ , is a linear combination of spatially translated and time-delay feedback terms. Specifically,

$$F = \rho[A(x + \Delta x, t) - A(x, t)] + \gamma[A(x, t) - A(x, t - \Delta t)], \quad (6)$$

where  $\gamma$  and  $\rho$  are real parameters and  $\Delta t > 0$ . Note that if a solution  $A(x, t)$  is spatially periodic with period  $L = \Delta x/n$ ,  $n \in \mathbb{Z}$  and temporally periodic with period  $T = \Delta t/m$ ,  $m \in \mathbb{Z}$ , the feedback term vanishes. Thus such a space and time periodic state is also a solution of the CGLE without feedback. We will restrict our linear stability analysis to traveling plane wave solutions (2) which have the same spatial and temporal scales as the feedback, *i.e.* we assume

$$\Delta x = 2\pi/K, \quad \Delta t = 2\pi/|\omega|. \quad (7)$$

Note that this choice of spatial feedback scale assumes that the targeted traveling wave state is not too close to bandcenter ( $K = 0$ ). The temporal feedback assumes  $\omega \neq 0$ , or equivalently  $K^2 \neq 1/(1 + b_1 b_3)$ .

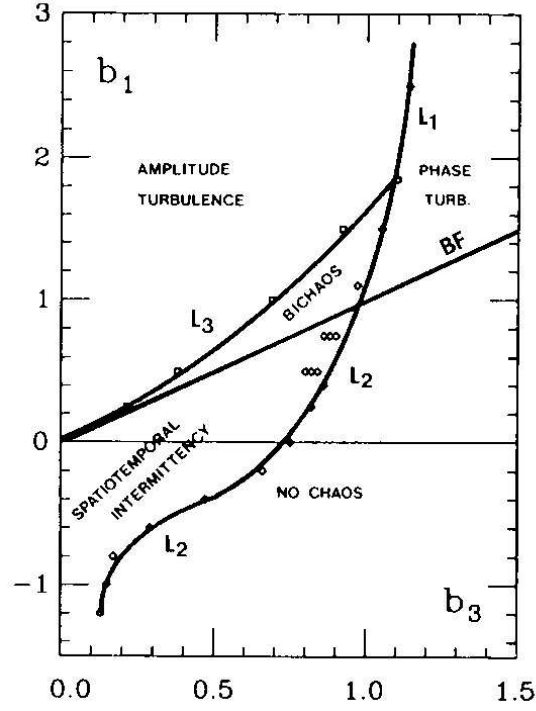


**Figure 1.** Phase diagram for the 1-D complex Ginzburg Landau equation (1) in the  $(b_3, b_1)$ -parameter plane. All plane wave solutions (2) are unstable above the Benjamin-Feir (BF) line  $b_1 = b_3$ . This figure is reproduced (with permission of the author) from [44].

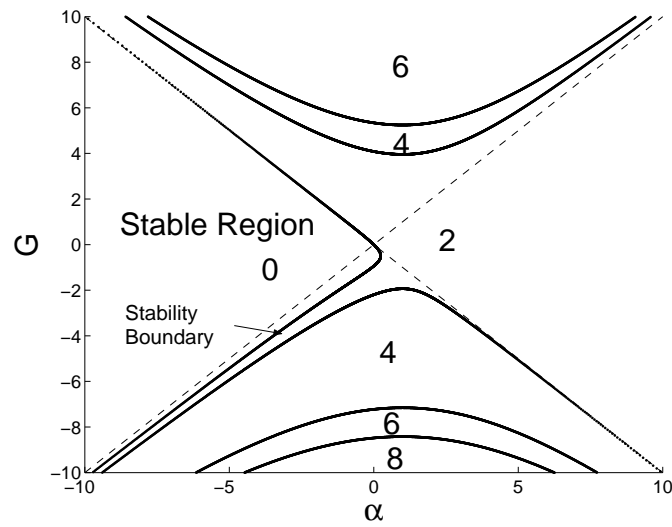


**Figure 2.** Example of critical curves (solid lines) in the  $(\alpha, G)$ -parameter plane of (8), given by (9), in the nondegenerate case  $\beta\Delta t \neq n\pi$  for any integer  $n$ . (Here we used  $\Delta t = 1$  and  $\beta = -4\pi/5$ .) The dashed lines are the asymptotes  $G = \pm\alpha$ . The numbers in the various regions indicate how many solutions of the characteristic equation (9) have positive real part. The stable region is to the left of all critical curves [40].

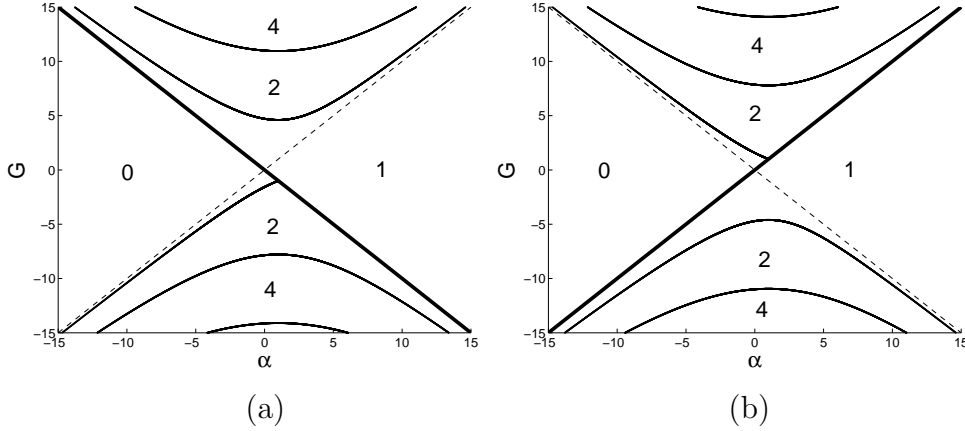


**Figure 3.** Examples of critical curves associated with (8) in the degenerate cases for which  $\beta\Delta t = n\pi$  for some integer  $n$ . (a)  $\Delta t = 1$ ,  $\beta = -\pi$  (representative of  $n$  odd). (b)  $\Delta t = 1$ ,  $\beta = -2\pi$  (representative of  $n$  even).

Our linear stability analysis builds on some results of Reddy *et al.* [40], who considered the effects of a time-delayed linear feedback term added to a Hopf bifurcation normal form. Of relevance to our analysis are their results on the linear stability of the origin, which is determined by an analysis of

$$\dot{z}(t) = (\alpha + i\beta)z(t) - Gz(t - \Delta t), \quad (8)$$

where  $\alpha$ ,  $\beta$ ,  $G$ ,  $\Delta t$  are real parameters with  $\Delta t > 0$ . The characteristic equation associated with solutions of the form  $z = e^{\lambda t/\Delta t}$  is

$$\lambda = (\alpha + i\beta)\Delta t - G\Delta t e^{-\lambda}. \quad (9)$$

There are an infinite number of solutions  $\lambda$  to this transcendental equation; if all of them satisfy  $\text{Re}(\lambda) < 0$ , then  $z = 0$  is stable. If any solution  $\lambda$  has positive real part, then  $z = 0$  is unstable. (See, for example, Diekmann *et al.* [45] or Driver [46] for background on delay equations.)

A solution  $\lambda$  of the characteristic equation is purely imaginary on the “critical curves” in the  $(\alpha, G)$ -parameter plane. These curves are significant because they represent boundaries in the  $(\alpha, G)$ -plane across which the number of solutions with  $\text{Re}(\lambda) > 0$  changes. Figure 2 shows an example of critical curves in the  $(\alpha, G)$ -plane, associated with a “nondegenerate case” for which  $\beta\Delta t \neq n\pi$  for any  $n \in \mathbb{Z}$ , with examples of critical curves for degenerate cases provided in Figure 3. A parameterization of the critical curves is obtained by letting  $\lambda = i\nu$ ,  $\nu \in \mathbb{R}$ , in (9), in which case we find

$$\begin{aligned} \alpha &= \frac{(\nu - \beta\Delta t) \cos(\nu)}{\Delta t \sin(\nu)}, \\ G &= \frac{(\nu - \beta\Delta t)}{\Delta t \sin(\nu)}. \end{aligned} \quad (10)$$

Here each critical curve is associated with an interval  $\nu \in (m\pi, (m+1)\pi)$  for some integer  $m$ . In the nondegenerate situation, Reddy *et al.* [40], extending a result in [45], show

that the stability boundary is determined by the left most critical curve in the  $(\alpha, G)$ -plane, as indicated in Figure 2. This stability boundary corresponds to the critical curve for the  $\nu$ -interval containing  $\beta\Delta t$ ; it passes through the origin and approaches the asymptotes  $G = \pm\alpha$  as  $\alpha \rightarrow -\infty$ . In the degenerate cases (Figure 3), defined by  $\beta\Delta t = n\pi$  for some integer  $n$ , there is an additional critical curve coincident with one of the asymptotes; specifically if  $n$  is even (odd) then on the critical curve  $\alpha = G$  ( $\alpha = -G$ ) the characteristic equation (9) is solved by  $\lambda = i\nu = i\beta\Delta t (= in\pi)$ . Finally, we show that the following properties hold for the critical curves in the nondegenerate case.

**Lemma 1.** *Consider  $G < 0$  and  $\beta\Delta t \neq n\pi$  for any  $n \in \mathbb{Z}$  in (8). (1) The stability boundary in the  $(\alpha, G)$ -parameter plane is the greatest distance from the asymptote  $\alpha = G$  for  $G = -\frac{1}{\Delta t}$ . (2) All other critical curves (to the right of the stability boundary and for  $G < 0$ ) lie in the region  $G < -\frac{1}{\Delta t}$ .*

*Proof.* (1) At a point where the distance between the stability boundary and the asymptote  $\alpha = G$  is maximized

$$\frac{d\alpha}{d\nu} = \frac{dG}{d\nu} ; \quad \frac{d^2G}{d\nu^2} - \frac{d^2\alpha}{d\nu^2} > 0 , \quad (11)$$

where  $\alpha(\nu)$  and  $G(\nu)$  are the parametric equations for the critical curves (10). It follows by direct calculation that these conditions are met when  $\nu = \nu^*$ , where  $\nu^*$  is defined implicitly by the equation

$$\sin(\nu^*) = \beta\Delta t - \nu^* . \quad (12)$$

From (10), we see that this implies  $G = -\frac{1}{\Delta t}$ . (It follows from property (2) of this lemma that  $\nu^*$  defines a point on the stability boundary rather than another critical curve.) (2) The remaining critical curves in the region  $G < 0$  reach their maximum in the  $(\alpha, G)$ -plane at points for which  $\frac{dG}{d\nu} = 0$  (while  $\frac{d\alpha}{d\nu} \neq 0$ ), where

$$\frac{dG}{d\nu} = \frac{\sin(\nu) - (\nu - \beta\Delta t) \cos(\nu)}{\Delta t \sin^2(\nu)} . \quad (13)$$

Substituting

$$\sin(\nu) = (\nu - \beta\Delta t) \cos(\nu) \quad (14)$$

into (10) yields

$$G_{max} = \frac{1}{\Delta t \cos(\nu)} \quad (15)$$

for the maximum value of  $G$ , where  $\nu$  satisfies (14). For the critical curves confined to  $G < 0$ ,  $-1 < \cos(\nu) < 0$  in (14) so  $G_{max} < -\frac{1}{\Delta t}$ .  $\square$



### 3. Linear Stability Analysis

#### 3.1. Preliminaries

In order to determine whether the feedback (6-7) can stabilize a traveling wave solution (2) of (5), we analyze the effects of small amplitude perturbations on the solution by letting

$$A = Re^{iKx+i\omega t}(1 + a_+(t)e^{iQx} + a_-(t)e^{-iQx}). \quad (16)$$

Here  $a_+$  and  $a_-$  are the amplitudes of small perturbations with wavenumbers  $K \pm Q$ . (We may, without loss of generality, assume that  $Q \geq 0$ .) Substituting (16) into (5) and linearizing, yields the following system of delay equations:

$$\frac{d}{dt} \begin{pmatrix} a_+(t) \\ a_-^*(t) \end{pmatrix} = J \begin{pmatrix} a_+(t) \\ a_-^*(t) \end{pmatrix} - \gamma \begin{pmatrix} a_+(t - \Delta t) \\ a_-^*(t - \Delta t) \end{pmatrix}, \quad (17)$$

where

$$J = \begin{bmatrix} \gamma - Q(2K + Q)(1 + ib_1) & -(b_3 - i)R^2 \\ -(b_3 - i)R^2 + \rho[e^{iQ\Delta x} - 1] & \\ & -(b_3 + i)R^2 \\ & \gamma + Q(2K - Q)(1 - ib_1) \\ & -(b_3 + i)R^2 + \rho[e^{iQ\Delta x} - 1] \end{bmatrix}. \quad (18)$$

Diagonalizing yields two decoupled linear delay equations,

$$\frac{d}{dt}c_k(t) = j_k c_k(t) - \gamma c_k(t - \Delta t), \quad k = 1, 2, \quad (19)$$

where  $j_1$  and  $j_2$  are the complex eigenvalues of  $J$  defined such that  $Re(j_1) \geq Re(j_2)$ .

Note that the temporal and spatial feedback terms, proportional to  $\gamma$  and  $\rho$ , simply shift the eigenvalues of  $J$  by the diagonal factor  $\gamma + \rho[e^{iQ\Delta x} - 1]$ . In particular, each  $j_k$  is of the form  $j_k = \gamma + \widehat{j}_k$ , where  $\widehat{j}_k$  is independent of  $\gamma$  and depends on  $b_1$ ,  $b_3$ ,  $\rho$ ,  $K$ , and  $Q$ . In the following we denote the real and imaginary parts of  $\widehat{j}_k$  by  $\widehat{j}_{kr}$  and  $\widehat{j}_{ki}$ , respectively. Since  $\widehat{j}_{1r}$  plays a central role in our analysis, we simplify notation by replacing it with  $f$  and suppressing its dependence on the system and solution parameters  $b_1, b_3, \rho, K$ , viewing it as a function of the perturbation parameter  $Q$ . Specifically, we let

$$f(Q) \equiv \widehat{j}_{1r}(Q; b_1, b_3, \rho, K) \equiv j_{1r}(Q; b_1, b_3, \rho, K, \gamma) - \gamma. \quad (20)$$

We note that  $f(Q)$  and  $j_{1i}(Q)$  are continuous functions of  $Q$ , and that  $f(Q)$  satisfies

$$\begin{aligned} f(0) &= 0, \\ \lim_{Q \rightarrow \infty} f(Q) &\rightarrow -\infty. \end{aligned} \quad (21)$$

Hence  $f(Q)$  has an absolute maximum  $f_{max} \geq 0$  for some  $Q \geq 0$ . The significance of  $f(Q)$  is that it represents the growth rate of perturbations of wavenumber  $Q$  in the absence of the time-delay feedback (*i.e.* for  $\gamma = 0$ ).

The characteristic equations associated with solutions  $c_k(t) = e^{\lambda_k t / \Delta t}$  of (19) are

$$\lambda_k = \Delta t(j_k - \gamma e^{-\lambda_k}), \quad k = 1, 2. \quad (22)$$

We obtain the critical curves associated with our linear stability problem (19) by substituting  $\lambda_k = i\nu_k$  into (22). Then, for instance, we find the following parametric representation of critical curves in the  $(j_{1r}, \gamma)$ -planes:

$$j_{1r} = \frac{(\nu_1 - j_{1i}\Delta t) \cos(\nu_1)}{\Delta t \sin(\nu_1)} \quad (23)$$

$$\gamma = \frac{(\nu_1 - j_{1i}\Delta t)}{\Delta t \sin(\nu_1)}. \quad (24)$$

Similar equations apply for the critical curves in the  $(j_{2r}, \gamma)$ -parameter plane. Using  $j_{1r} = \gamma + f(Q)$  (which, recall, defines  $f(Q)$ ) we determine that on the critical curves in the  $(j_{1r}, \gamma)$ -plane  $Q$  and  $\nu_1$  are related through

$$f(Q)\Delta t = w(\nu_1, Q), \quad (25)$$

where

$$w(\nu_1, Q) \equiv \frac{(\nu_1 - j_{1i}(Q)\Delta t)(\cos(\nu_1) - 1)}{\sin(\nu_1)}, \quad (26)$$

which is a result we use later in our analysis.

The parametric equations for the critical curves (23-24) in the  $(j_{1r}, \gamma)$ -plane are similar to those obtained by Reddy *et al.* [40], given by (10). However since both  $j_{1r}$  and  $j_{1i}$  depend on the perturbation wavenumber  $Q$  the results in [40], summarized by Figures 2 and 3, do not apply directly. Nonetheless some useful results concerning the stability boundary do carry over. For instance, it follows from (23) and (24) that  $j_{1r} = \gamma \cos(\nu)$  so all critical curves must lie in the region of the  $(j_{1r}, \gamma)$ -plane where  $|j_{1r}| \leq |\gamma|$ . In other words, if we divide the  $(j_{1r}, \gamma)$ -plane into four quadrants separated by  $\gamma = \pm j_{1r}$  the critical curves lie inside (or possibly on the boundaries) of the upper and lower quadrants (as is also the case in Figures 2 and 3). The stability assignments are necessarily the same at all points inside the left and right quadrants of the parameter plane. In particular, the left quadrant is contained in the stable region and the right quadrant is contained in the unstable region for all  $j_{1i}$ . Because the stability boundary is contained in the upper and lower quadrants both stable and unstable regions are located there, as signified by the question marks in Figure 4. For fixed values of  $b_1$ ,  $b_3$ ,  $K$ , and  $\rho$ , the quadrants of the  $(j_{1r}, \gamma)$ -plane may be mapped to the  $(Q, \gamma)$ -plane. In particular, the asymptotes  $\gamma = \pm j_{1r}$  are mapped to the curves defined by  $f(Q) = 0$  and  $\gamma = -f(Q)/2$ ; an example is shown in Figure 4.

We note that due to the translation symmetry of (5), which acts nontrivially on the traveling wave solution (2), there is always a neutral mode associated with perturbations at  $Q = 0$ . (It is this symmetry that forces  $f(0) = 0$ .) Thus the line  $j_{1r} = \gamma$  is a (degenerate) critical curve; as it is a consequence of translation symmetry, it does not necessarily herald an instability.

We now make use of the elementary (in)stability results summarized by Fig. 4(a) to prove Lemmas 2–3, which allow us to restrict any further linear stability analysis to the  $k = 1$  delay equation of (19) for  $Q > 0$ , and for feedback parameters  $\gamma < 0$  and

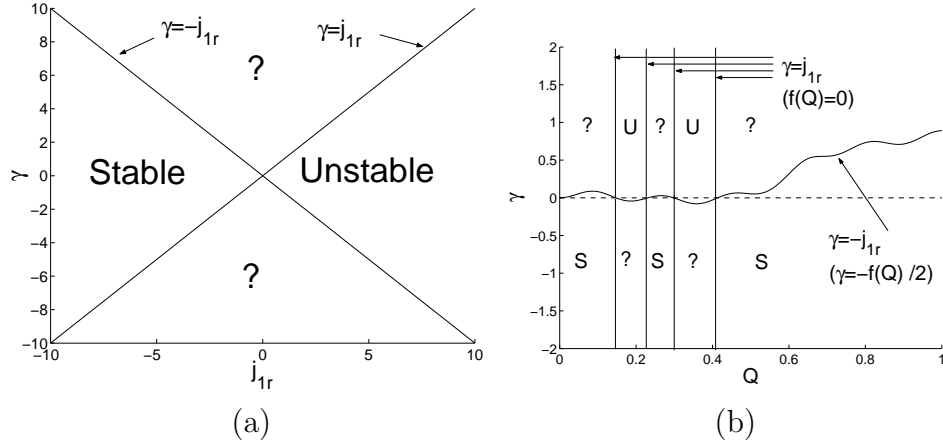


**Figure 4.** Mapping of the guaranteed stable (S) and unstable (U) regions bounded by  $\gamma = \pm j_{1r}$  from (a) the  $(j_{1r}, \gamma)$ -plane to (b) the  $(Q, \gamma)$ -plane. The parameter values are  $b_1 = 5$ ,  $b_3 = 1.2$ ,  $K = 0.18$ , and  $\rho = 0.1$ .

$\rho \geq 0$ . In particular, we find that the restriction  $\gamma < 0$ ,  $\rho > 0$  is sufficient to ensure that the feedback does not further destabilize the traveling waves in the Benjamin-Feir unstable regime, *i.e.* the feedback does not introduce new instabilities in this case.

**Lemma 2.** (a) If  $f(Q) < 0$  for all  $Q > 0$ , where  $f(Q)$  is defined by the relation (20), then the traveling wave is stabilized for any  $\gamma \leq 0$ . In particular, the wave is stabilized using spatial feedback alone in (6) (*i.e.* for  $\gamma = 0$ ), and there are no instabilities associated with  $Q = 0$  when  $\gamma \leq 0$ . (b) If  $f(Q) > 0$  for any  $Q$  then the traveling wave cannot be stabilized using  $\gamma \geq 0$ .

*Proof.* (a) If  $f(Q) < 0$ , then  $j_{2r} \leq j_{1r} < \gamma$  for all  $Q > 0$  since  $j_{1r} = \gamma + f(Q)$ . Hence, for  $\gamma \leq 0$ , the system is in the guaranteed stable regime of Fig. 4(a) for all perturbations with  $Q > 0$ . It remains to eliminate the possibility of instabilities at  $Q = 0$ , where  $j_{2r}(0) < j_{1r}(0) = \gamma$ . For this we consider the solutions  $\lambda_k = \mu_k + i\nu_k$  of the characteristic equation (22), and determine that the growth rates  $\mu_k$  satisfy

$$\mu_k = \Delta t \left( \widehat{j_{kr}} + \gamma(1 - e^{-\mu_k} \cos(\nu_k)) \right). \quad (27)$$

There are no  $\mu_k > 0$  solutions of (27) when  $\gamma \leq 0$  and  $\widehat{j_{kr}} \leq 0$ . This is proved by assuming there is a solution with  $\mu_k > 0$ , which would imply that the left- and right-hand-sides of (27) do not have the same sign, thereby leading to a contradiction. In fact, the only solution with  $\mu_k = 0$  is the one forced by translation symmetry. Hence there can be no linear instabilities associated with  $Q = 0$  when  $\gamma \leq 0$ .

(b) If  $\gamma > 0$  and  $f(Q) > 0$  for some  $Q$ , then the system is in the guaranteed unstable regime of Fig. 4, defined by  $\gamma > -\frac{1}{2}f(Q)$ ,  $f(Q) > 0$ , for perturbations with that wavenumber. If there is no temporal feedback ( $\gamma = 0$ ) and  $f(Q) > 0$  for some  $Q$ , then instability for these  $Q$  values follows directly from the  $c_1(t)$  equation of (19), which

is

$$\frac{dc_1}{dt} = (f(Q) + ij_{1i})c_1 \quad \text{for } \gamma = 0 . \quad (28)$$

□

Lemma 2 motivates our focus on  $\gamma < 0$  in the remainder of the paper: if the time–delay feedback is to be effective in stabilizing plane waves, then the value of  $\gamma$  used in (6) should be negative. We similarly focus on  $\rho \geq 0$ . This is because the spatial feedback has the effect of shifting each  $j_{kr}$  in (27) by  $\rho[\cos(Q\Delta x) - 1]$ . Thus there is no effect of the spatial feedback on perturbations with wavenumber  $Q = 2n\pi/\Delta x$  for some  $n \in \mathbb{Z}$ . And, for all other wavenumbers, there is a shift towards the stable region of Figure 4(a) if  $\rho > 0$  and towards the unstable region if  $\rho < 0$ . In particular, in the absence of time–delay feedback, if  $\rho < 0$  the spatial feedback exacerbates longwave instabilities in the Benjamin–Feir unstable regime. In the remainder of the paper we consider only  $\rho \geq 0$ . In this case, as explained by the following lemma, we may ignore the  $c_2$ –equation of (19) in the remainder of our linear stability analysis.

**Lemma 3.** *If  $\gamma \leq 0$  and  $\rho \geq 0$  in (19) then all solutions of the  $c_2$ –equation of (19) decay exponentially.*

*Proof.* The real parts of the eigenvalues  $j_k$  of the matrix  $J$  (18), can be written in the form

$$j_{1r} = a + \gamma + |p| , \quad j_{2r} = a + \gamma - |p| \quad (29)$$

since they are solutions of a quadratic. From (18) it follows that

$$a = -\left(Q^2 + b_3 R^2 + \rho[1 - \cos(Q\Delta x)]\right), \quad (30)$$

so  $a < 0$  for  $\rho \geq 0$ . Thus

$$j_{2r} - \gamma = a - |p| < 0 \quad (31)$$

for all values of  $Q$  and  $\rho \geq 0$ . From Fig. 4(a) (with  $j_{2r}$  replacing  $j_{1r}$ ) we see that the parameters are in the guaranteed stable region when  $\gamma < 0$ . Finally, if  $\gamma = 0$ , then the  $c_2$ –equation reduces to

$$\frac{d}{dt}c_2 = \widehat{j_2}c_2 \quad \text{for } \gamma = 0 , \quad (32)$$

so all solutions decay for  $\gamma = 0$  since  $\widehat{j_2} = a - |p| < 0$ . □

### 3.2. Main Stability Results

Lemma 2 states that if  $f(Q)$ , defined by (20), is negative for all  $Q > 0$ , then the traveling wave may be stabilized using spatial feedback alone ( $\gamma = 0$ ). This section addresses the more difficult case where the chosen spatial feedback fails to stabilize the traveling wave, *i.e.*, we consider the situation where  $f(Q) > 0$  for some range of  $Q$  values and investigate whether the traveling waves may then be stabilized by the addition of an appropriate time-delay feedback with  $\gamma < 0$ . (From Lemma 2 we know that the wave cannot be stabilized with  $\gamma > 0$ .) We focus on the case where the spatial feedback parameter  $\rho$  is fixed at some non-negative value so that Lemma 3 applies. We show that it is then sufficient to consider just  $\gamma = -1/\Delta t$  in order to determine whether or not the traveling waves can be stabilized by including the time-delay feedback in (6).

Our analysis relies on the observation that not all regions of the  $(j_{1r}, \gamma)$ -parameter plane are accessible for fixed  $b_1, b_3, K, \rho$  and  $Q \geq 0$ . In particular, since  $j_{1r} = \gamma + f(Q)$  and  $f(Q)$  has an absolute maximum (denoted by  $f_{max}$ ), parameter values to the right of the line

$$\gamma = j_{1r} - f_{max} \quad (33)$$

are never achieved for any value of  $Q$  (see Figure 5). We refer to the boundary (33) between accessible and inaccessible regions of the  $(j_{1r}, \gamma)$ -parameter plane as the “existence line”, meaning that there *exist* values of  $Q$  that place  $j_{1r}$  and  $\gamma$  on or to the left of this line, but never to the right of it. Our stability analysis focuses on determining whether there is a (negative)  $\gamma$ -value such that the traveling wave is stable for all values of  $j_{1r}$  between  $-\infty$  and the existence line, *i.e.* for all values of  $Q$ . Fig. 6 presents, schematically, projections onto the  $(j_{1r}, \gamma)$ -plane of the points that lie on the stability boundary in the three-dimensional  $(j_{1r}(Q), \gamma, j_{1i}(Q))$  parameter space. Figure 6(a) typifies the case where it is possible to stabilize the traveling wave over the range of  $\gamma$ -values for which the stability boundary leaves the existence region. On the other hand, in Fig. 6(b) the stability boundary lies entirely to the left of the existence line for all values of  $\gamma$  so it is not possible to stabilize the traveling wave in this case.

We now state our main linear stability result; the proof, which relies on Lemma 8 below, is deferred to the end of this section.

**Theorem 1.** *The traveling wave solution (2) of the CGLE (1) with feedback (6-7) may be (linearly) stabilized, for a fixed given value of  $\rho \geq 0$ , if and only if the following equations fail to have a real solution  $(\nu, Q)$ ,  $Q > 0$ :*

$$\nu + \sin(\nu) = \Delta t \, j_{1i}(Q) \quad (34)$$

$$1 - \cos(\nu) = \Delta t \, f(Q) . \quad (35)$$

*If a solution fails to exist then the traveling wave can be stabilized using  $\gamma = -1/\Delta t$ .*

**Remark 1:** Note that any solution of (35) that exists must lie in a closed interval of  $Q$  values defined by the requirement  $f(Q)\Delta t \in [0, 2]$ .

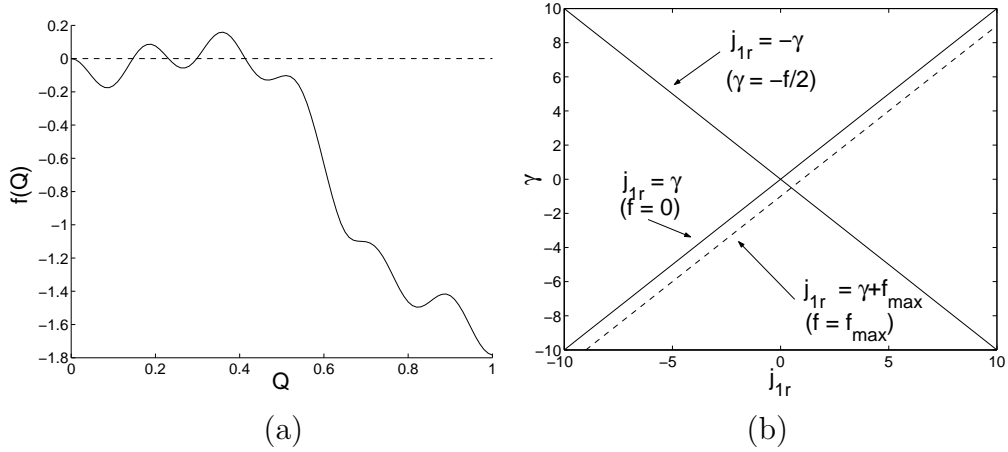


**Figure 5.** (a) Plot of  $f(Q)$  for the parameters of Figure 4. (b) Corresponding regions of the  $(j_{1r}, \gamma)$ -parameter plane (where  $j_{1r} = \gamma + f(Q)$ );  $j_{1r}$  values to the right of the existence line (33) are inaccessible.

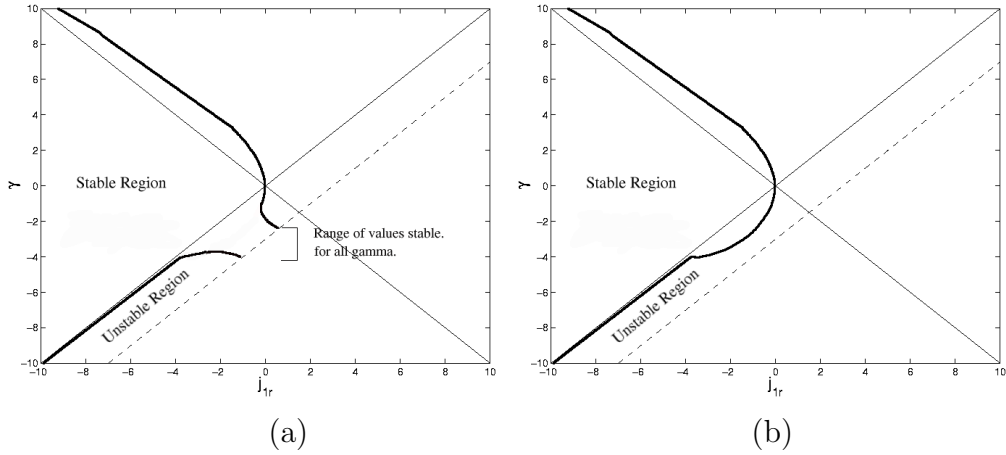


**Figure 6.** (a) Schematic of stable region for case that the stability boundary leaves the existence region. Range of  $\gamma$  values for which the traveling wave is stable against perturbations of all wavenumber  $Q$  is indicated. (b) Schematic of the unstable case where the stability boundary lies to the left of the existence line for all  $\gamma$ .

**Remark 2:** Equations (34–35) are equivalent to the equations for the critical curves (23–24) for  $\gamma = -1/\Delta t$  and  $\nu_1 = \nu$ .

The following lemma addresses special degenerate situations for which stabilization of the traveling wave is impossible.

**Lemma 4.** *Let  $Q = Q_{2n} > 0$  be defined by the condition that  $j_{1i}(Q_{2n})\Delta t = 2\pi n$ ,  $n \in \mathbb{Z}$ . The traveling wave solution (2) of the CGLE (1) with feedback (6–7) is linearly unstable for all values of  $\gamma$  if for any  $n$  (a)  $f(Q_{2n}) > 0$ , or (b)  $f(Q_{2n}) = 0$  and  $\frac{df}{dQ}(Q_{2n}) \neq 0$ . (c) If  $f(Q_{2n}) = \frac{df}{dQ}(Q_{2n}) = 0$ , then the traveling wave is either linearly unstable or neutrally stable; it is not linearly stable for any value of  $\gamma$ .*

*Proof.* (a) In the degenerate situation, for the value of  $Q = Q_{2n}$ , where  $j_{1i}(Q_{2n})\Delta t = 2\pi n$  ( $n \in \mathbb{Z}$ ), the line  $j_{1r} = \gamma$  represents a critical curve for the delay equation (19) (with

$k = 1$ ). (Here we are viewing  $j_{1r}$  as an independent parameter, with  $j_{1i}$  held fixed; see Fig. 3(b) with  $\alpha = j_{1r}$  and  $G = \gamma$ .) Thus the traveling wave solution is unstable to perturbations with wavenumber  $Q = Q_{2n}$  if  $j_{1r}(Q_{2n}) > \gamma$ . Since  $f(Q) \equiv j_{1r}(Q) - \gamma$ , this inequality is met whenever  $f(Q_{2n}) > 0$ .

(b) If  $f(Q_{2n}) = 0$ , then  $j_{1r}(Q_{2n}) = \gamma$  and the solution is neutrally stable to perturbations of wavenumber  $Q = Q_{2n}$  for  $\gamma \leq 0$ . (It is unstable if  $\gamma > 0$  since it lies in the guaranteed unstable regime of Fig. 4(a)) To determine the stability of the traveling wave for  $\gamma < 0$  we examine the movement, with  $Q$ , of the solutions  $\lambda_1 = \mu_1 + i\nu_1$  of the characteristic equation (22). From the real and imaginary parts of (22) we have

$$\mu_1 = f(Q)\Delta t + \gamma\Delta t - \gamma\Delta t e^{-\mu_1} \cos(\nu_1), \quad (36)$$

$$\nu_1 = j_{1i}(Q)\Delta t + \gamma\Delta t e^{-\mu_1} \sin(\nu_1), \quad (37)$$

which has solution  $\mu_1 = 0$ ,  $\nu_1 = j_{1i}(Q_{2n})\Delta t = 2\pi n$  for  $Q = Q_{2n}$ . To determine the movement of  $\mu_1$  with  $Q$  near  $Q_{2n}$ , we compute  $\frac{d\mu_1}{dQ}(Q_{2n})$ . We find

$$\frac{d\mu_1}{dQ}(Q_{2n}) = \frac{\Delta t}{1 - \gamma\Delta t} \frac{df}{dQ}(Q_{2n}) \neq 0. \quad (38)$$

Since  $\frac{\Delta t}{1 - \gamma\Delta t} > 0$  for  $\gamma < 0$ , the eigenvalue  $\lambda_1$  moves into the unstable region  $\mu_1 > 0$  with increasing (decreasing)  $Q$  if  $\frac{df}{dQ}(Q_{2n}) > 0$  ( $< 0$ ).

(c) If  $f(Q_{2n}) = \frac{df}{dQ}(Q_{2n}) = 0$ , then the traveling wave may only be neutrally stable for  $\gamma \leq 0$ . This latter claim follows since the critical eigenvalue  $\lambda_1(Q_{2n}) = 2\pi n$  does not cross the imaginary axis with finite speed as  $Q$  is varied near  $Q_{2n}$ , *i.e.*  $\frac{d\mu_1}{dQ}(Q_{2n}) = 0$ . This tangency implies that the traveling wave cannot be linearly stable in this case – it is either unstable or “at best” neutrally stable.  $\square$

A consequence of this lemma is that the temporal feedback cannot be used to stabilize homogeneous oscillations. (Note that for  $K = 0$ , spatial feedback is not applicable and only the temporal feedback is relevant.) Specifically, for  $K = \rho = 0$ , the matrix  $J$ , given by (18), has eigenvalues that are purely real for  $Q$  sufficiently small and hence we have  $j_{1i}(Q) = 0$  with  $f(Q) > 0$  for sufficiently longwave perturbations associated with the Benjamin-Feir unstable regime. It follows immediately from Lemma 4 (with  $n = 0$ ), that the feedback fails to stabilize the uniform oscillatory mode associated with  $K = 0$ . In this context, we note that Beta *et al.* [29] have given a possible physical explanation for the failure of time-delayed global feedback to stabilize a uniform oscillatory mode in the case of diffusion-induced chemical turbulence. Harrington and Socolar [18] have a related result that shows that time-delay feedback alone cannot stabilize traveling wave solutions of the two-dimensional CGLE.

We may further interpret Lemma 4 in light of analogous results for the spatial feedback. Specifically, we recall that the effect of the spatial feedback on the eigenvalues of the matrix  $J(Q)$ , given by (18), is to shift them by the diagonal entry  $\rho(e^{iQ\Delta x} - 1)$ . Thus if there is an unstable wavenumber  $Q = \tilde{Q}_n$  for which  $\tilde{Q}_n\Delta x = 2n\pi$  for some integer  $n$ , then the spatial feedback can have no stabilizing effect on that perturbation

wavenumber. In this case, the perturbation wavenumber  $\tilde{Q}_n$  is “resonant” with the underlying wavenumber  $K$  of the traveling wave ( $\tilde{Q}_n = nK$ ), and it does not feel the influence of the feedback. Lemma 4 leads to an analogous result when the frequency associated with the perturbation at  $Q_{2n}$ , namely  $j_{1i}(Q_{2n})$ , is in resonance with the temporal delay  $\Delta t$ , *i.e.*  $j_{1i}(Q_{2n})\Delta t$  happens to also be an even multiple of  $\pi$ . In that case, the temporal feedback term also has no effect on the perturbation, *i.e.* it cannot suppress the instability associated with it. Just *et al.* [32] refer to such situations where the method of Pyragas fails as “torsion-free”. These observations about special (nongeneric) spatial *and* temporal resonant cases are summarized by the following corollary to Lemma 4.

**Corollary 1.** *If, in the absence of any feedback ( $\gamma = \rho = 0$ ), there is an unstable wavenumber  $Q = \tilde{Q}$  for which  $\tilde{Q}\Delta x = 2m\pi$  and  $j_{1i}(\tilde{Q})\Delta t = 2n\pi$  for some integers  $m$  and  $n$ , then the traveling wave cannot be stabilized using the feedback (6) for any value of  $\rho$  or  $\gamma$ .*

**Remark:** It follows from (7) that the resonance conditions  $\tilde{Q}\Delta x = 2m\pi$  and  $j_{1i}(\tilde{Q})\Delta t = 2n\pi$  are equivalent to the conditions  $\tilde{Q} = mK$  and  $j_{1i}(\tilde{Q}) = n\omega$ , respectively.

It now remains to consider whether stabilization is possible when  $j_{1i}(Q)\Delta t \neq 2\pi n$  for any  $n \in \mathbb{Z}$  over all intervals of  $Q$  for which  $f(Q) > 0$ . It is consideration of this situation that leads to the stabilization criterion of Theorem 1. In particular, we aim to determine a necessary and sufficient condition for the stability boundary in the  $(j_{1r}, \gamma)$ -plane to be parameterized by  $Q$ , such that it extends *continuously* from the origin to  $\gamma \rightarrow -\infty$  along the asymptote  $\gamma = j_{1r}$ , as in Fig. 6(a). Hence we focus on the mapping (25–26) between  $Q$  and  $\nu_1$  along the critical curves.

We first describe some properties of the function  $w(\nu_1, Q)$ , given by (26), for fixed  $Q$ . In particular, we are interested in this function over the interval of  $\nu_1$ -values that parameterizes the stability boundary in the  $(j_{1r}, \gamma)$ -plane in the case where  $j_{1r}$  is allowed to vary independently of  $j_{1i}$ , which is held fixed with  $j_{1i}\Delta t \neq 2\pi n$  in (23–24). Our first lemma treats the case where  $j_{1i}\Delta t \neq n\pi$  for any  $n \in \mathbb{Z}$ , while the second lemma describes the degenerate case  $j_{1i}\Delta t = (2n + 1)\pi$  for some  $n \in \mathbb{Z}$ . Each lemma consists of two parts: the first part merely defines the interval of  $\nu_1$ -values that parameterizes the stability boundary in each  $(j_{1r}, \gamma)$ -plane ( $j_{1i}$  fixed) and the second part describes  $w(\nu_1, Q)$  on that interval. The first part of each lemma follows directly from the analysis of Reddy *et al.* [40], described in Section 2.

**Lemma 5.** *Consider  $\gamma < 0$  and let  $j_{1r}$  in (23–24) vary independently of  $j_{1i}$ , which is held fixed with  $j_{1i}\Delta t \neq n\pi$  for any  $n \in \mathbb{Z}$ . (1) The stability boundary in the  $(j_{1r}, \gamma)$ -plane is associated with an interval  $I_\nu = (\nu_a, \nu_b)$  of  $\nu_1$ -values. The endpoints,  $\nu_a$  and  $\nu_b$ , are  $j_{1i}\Delta t$  and  $2\pi n$ , where  $n \in \mathbb{Z}$  is chosen so that  $|j_{1i}\Delta t - 2\pi n| < \pi$ . (2) For  $\nu_1 \in I_\nu$  the function  $w(\nu_1, Q)$  (with  $Q$  fixed) is positive with  $w(\nu_1, Q) \rightarrow 0$  as  $\nu_1$  approaches  $\nu_a$  and  $\nu_b$ ;  $w(\nu_1, Q)$  has a unique maximum value  $w_{max}(Q)$  at  $\nu_1 = \nu^*$ , where*

$$\sin(\nu^*) = j_{1i}(Q)\Delta t - \nu^* , \quad w_{max}(Q) = 1 - \cos(\nu^*) . \quad (39)$$



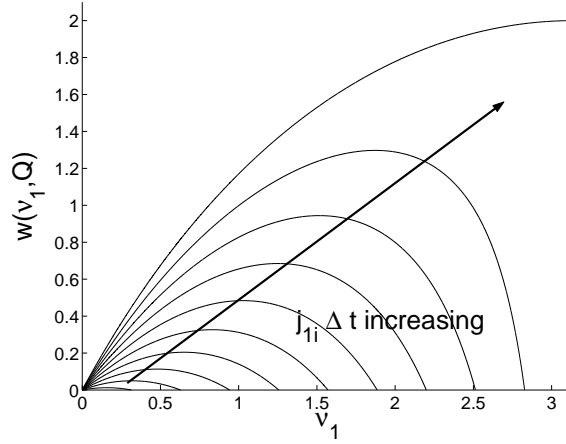


**Figure 7.** Plots of  $w(\nu_1, Q)$  vs.  $\nu_1$ , where  $w$  is defined by (26), for various (fixed) values of  $Q$  such that  $j_{1i}\Delta t \in (0, \pi]$ .

*Proof.* From Reddy *et al.* [40], we have that the stability boundary (for  $\gamma < 0$ ) extends between the origin of the  $(j_{1r}, \gamma)$ -plane and the asymptote  $\gamma = j_{1r}$  as  $\gamma \rightarrow -\infty$ . The boundary is associated with an open interval  $I_\nu$ ; the endpoints of the interval correspond to  $j_{1i}\Delta t$  (at the origin) and the nearest value of  $2\pi n$  (as  $\gamma \rightarrow -\infty$ ). In particular, the following two possibilities follow from the parameterization (23-24): (a) there exists an  $n \in Z$  such that  $j_{1i}\Delta t - 2\pi n < \pi$  in which case  $I_\nu = (2\pi n, j_{1i}\Delta t)$ , or (b) there exists an  $n \in Z$  such that  $2\pi n - j_{1i}\Delta t < \pi$  in which case  $I_\nu = (j_{1i}\Delta t, 2\pi n)$ . In both cases it is straightforward to show that  $w(\nu, Q)$ , given by (26), is positive on the interval, approaching 0 at the endpoints  $2\pi n$  and  $j_{1i}\Delta t$ .

For fixed  $Q$ , we find the maximum of  $w(\nu_1, Q)$  on  $I_\nu$  by examining

$$\frac{\partial w(\nu_1, Q)}{\partial \nu_1} = \frac{(j_{1i}(Q)\Delta t - \nu_1 - \sin(\nu_1))}{(1 + \cos(\nu_1))}. \quad (40)$$

For  $\nu_1 \in I_\nu$ , the denominator on the right-hand-side of (40) is positive and the numerator is a decreasing function of  $\nu_1$  which goes through zero at  $\nu_1 = \nu^*$ , where  $\nu^*$  is defined implicitly by (39). The solution  $\nu^*$  of  $\frac{\partial w}{\partial \nu_1} = 0$  is unique and corresponds to a maximum of  $w$  on the interval  $I_\nu$ . In particular, it follows from (40) that  $w(\nu_1, Q)$  is increasing for  $\nu_1 \in (\nu_a, \nu^*)$  and decreasing for  $\nu_1 \in (\nu^*, \nu_b)$ . (See Figure 7 for sample plots of  $w(\nu_1, Q)$  on  $I_\nu$ ).  $\square$

**Lemma 6.** Consider  $\gamma < 0$  and let  $j_{1r}$  in (23-24) vary independently of  $j_{1i}$ , which is held fixed with  $j_{1i}\Delta t = (2n+1)\pi$  for some  $n \in Z$ . (1) The stability boundary in the  $(j_{1r}, \gamma)$ -plane consists of the line segment  $\gamma = -j_{1r}$  for  $\gamma \in (0, -\frac{1}{\Delta t}]$  and the parameterized curve (23-24) obtained (equivalently) with either the interval  $I_\nu^- \equiv (2n\pi, (2n+1)\pi)$  or  $I_\nu^+ \equiv ((2n+1)\pi, 2(n+1)\pi)$ . (2) For  $\nu_1 \in I_\nu^\pm$   $w(\nu_1, Q)$  is a positive function, with  $w \rightarrow 0$  as  $\nu_1 \rightarrow 2m\pi$  ( $m = n, m = (n+1)$  for  $I_\nu^-, I_\nu^+$ , respectively), and  $w$  approaches its maximum value  $w_{max} = 2$  as  $\nu_1 \rightarrow (2n+1)\pi$ . The function  $w(\nu_1, Q)$  on  $I_\nu^-$  is mapped

to  $w(\nu_1, Q)$  on  $I_\nu^+$  under the reflection  $\nu \rightarrow 2(2n+1)\pi - \nu$ . It is an increasing function on  $I_\nu^-$  and hence a decreasing function on  $I_\nu^+$ .

*Proof.* (1) In the degenerate case  $j_{1i}\Delta t = (2n+1)\pi$ , the line  $\gamma = -j_{1r}$  is a critical curve which forms the stability boundary for  $\gamma \geq -\frac{1}{\Delta t}$ ; see Fig. 3(a). This part of the stability boundary meets another critical curve at  $j_{1r} = -\gamma = \frac{1}{\Delta t}$ ; this follows from considering (23-24) in the limit  $\nu_1 \rightarrow (2n+1)\pi$ . The latter critical curve extends to  $j_{1r}, \gamma \rightarrow -\infty$  along  $\gamma = j_{1r}$  in the limit  $\nu_1 \rightarrow 2n\pi, 2(n+1)\pi$ . That the  $\nu_1$ -intervals  $I_\nu^-$  and  $I_\nu^+$  map out the same curve in the  $(j_{1r}, \gamma)$ -plane follows from the reflection symmetry of (23-24) under  $\nu \rightarrow 2j_{1i}\Delta t - \nu$  for  $j_{1i}\Delta t = (2n+1)\pi$ . This symmetry is also necessarily manifest in  $w(\nu_1, Q)$ .

(2) The proof of the other claims about  $w(\nu_1, Q)$  on  $I_\nu^\pm$  for  $j_{1i}\Delta t = (2n+1)\pi$  are straightforward. We note that the monotonicity of  $w(\nu_1, Q)$  on  $I_\nu^\pm$  is determined by (40). In particular, for  $j_{1i}\Delta t = (2n+1)\pi$ , there is a unique zero of  $\frac{\partial w}{\partial \nu_1}$  at  $\nu_1 = (2n+1)\pi$ , which corresponds to a maximum of  $w(\nu_1, Q)$  on the interval  $(2n\pi, 2(n+1)\pi)$ . Thus  $w(\nu_1, Q)$  is an increasing function on  $I_\nu^-$ , while it is decreasing on the interval  $I_\nu^+$ .  $\square$

We may now appreciate the relationship between  $\nu_1$  and  $Q$  along the stability boundary by considering the following procedure: for each  $Q$  for which  $f(Q) > 0$  calculate  $j_{1i}(Q)$  and  $f(Q)$  and then plot the left and right hand sides of (25) as functions of  $\nu_1$  over the appropriate interval  $I_\nu$  to determine which (if any)  $\nu_1$  values correspond to each value of  $Q$ . The left-hand-side of (25) yields a horizontal line with positive intercept. If  $j_{1i}(Q)\Delta t \neq n\pi$ , then by Lemma 5, the right-hand-side of (25), given by (26), is a positive function with a unique maximum (and no other critical points) over  $I_\nu$ ; see Fig. 7 for an example. Hence, in this case, there are either 0, 1, or 2 values of  $\nu_1$  associated with each  $Q$ . In this nondegenerate case we characterize the number of intersections of the curves associated with the left- and right-hand-sides of (25) over the interval  $I_\nu$  by determining whether the following distance function is positive (no intersections), zero (1 intersection) or negative (two intersections):

$$D(Q) = f(Q)\Delta t - w_{\max}(Q) , \quad (41)$$

where  $w_{\max}(Q)$  is given by (39). We note that  $D(Q)$  is continuous. This follows from the continuity of  $f(Q)$  and  $j_{1i}(Q)$ . In particular, since  $j_{1i}(Q)$  is continuous, the unique solution  $\nu^*$  of (39) is continuous in  $Q$ , thereby ensuring the continuity of  $w_{\max}(Q)$ .

For the degenerate cases prescribed by  $Q = Q_m$ , where  $Q_m$  is defined by  $j_{1i}(Q_m)\Delta t = m\pi$ , we define

$$w(\nu_1 = m\pi, Q_m) \equiv \lim_{\nu_1 \rightarrow m\pi} w(\nu_1, Q_m) = 1 - (-1)^m . \quad (42)$$

This corresponds to  $w_{\max}(Q_m)$ , which is 2 for odd  $m$  and 0 for even  $m$ . We now address the case that  $m$  is odd, i.e.  $m = 2n+1$  for some  $n \in \mathbb{Z}$ , in which case  $w(\nu_1, Q_{2n+1})$  is a positive function on the interval  $(2n\pi, 2(n+1)\pi)$ , and it is symmetric about  $\nu_1 = (2n+1)\pi$ . Thus, for  $Q = Q_{2n+1}$  defined by  $j_{1i}(Q_{2n+1})\Delta t = (2n+1)\pi$ , it follows from Lemma 6 that there are either no solutions or one solution of (25) for

$\nu_1 \in (2n\pi, (2n+1)\pi]$  or, equivalently, for  $\nu_1 \in [(2n+1)\pi, (2n+2)\pi)$ . We recall that in this degenerate case there is always an additional point on the stability boundary for  $\gamma = -f(Q_{2n+1})/2$  provided  $0 < f(Q_{2n+1})\Delta t < 2$ ; this point lies at the intersection of the lines  $j_{1r} = -\gamma$  and  $j_{1r} = \gamma + f(Q_{2n+1})$  (see part (1) of Lemma 6). Moreover, the condition  $0 < f(Q_{2n+1})\Delta t < 2$  is equivalent to  $f(Q_{2n+1})\Delta t < w_{\max}(Q_{2n+1})$  since  $w_{\max} = 2$  in this case. Thus the interpretation of the sign of  $D(Q)$ , defined by (41), is the same in this degenerate case as it is in the nondegenerate case. Specifically, if  $D(Q_{2n+1}) < 0$  then there are two points on the stability boundary associated with this value of  $Q_{2n+1}$ ; if  $D(Q_{2n+1}) = 0$ , then there is a single point on the stability boundary (given by  $(j_{1r}, \gamma) = (1/\Delta t, -1/\Delta t)$ ); and if  $D(Q_{2n+1}) > 0$ , then there are no points on the stability boundary associated with this value of  $Q_{2n+1}$ .

The next lemma addresses the continuity of particular critical curves that are parameterized by  $Q$ . It is specifically concerned with the case that  $j_{1i}(Q)\Delta t = (2n+1)\pi$  ( $n \in \mathbb{Z}$ ) at some point along the curve. At such points the relevant interval  $I_\nu$  of  $\nu_1$ -values may “jump” (e.g. from  $I_\nu^-$  to  $I_\nu^+$  in the case that  $Q = Q_{2n+1}$ ). However, this does not lead to a corresponding discontinuity in the critical curve parameterized by  $Q$ , as we now show.

**Lemma 7.** *Consider a critical curve in the  $(j_{1r}, \gamma)$ -plane, parameterized by  $Q$ , which extends from the origin to  $\gamma \rightarrow -\infty$  along the asymptote  $\gamma = j_{1r}$ . The critical curve is continuous at any points along it that are parameterized by  $Q = Q_{2n+1}$ , where  $j_{1i}(Q_{2n+1})\Delta t = (2n+1)\pi$  for some integer  $n$ , and  $f(Q_{2n+1})\Delta t \in (0, 2)$ .*

*Proof.* Let  $Q_{2n+1}$  be in the set of  $Q$  values that parameterizes the critical curve in the  $(j_{1r}, \gamma)$ -plane, where  $Q_{2n+1}$  is defined by the condition  $j_{1i}(Q_{2n+1})\Delta t = (2n+1)\pi$  for some integer  $n$ . Provided  $f(Q_{2n+1})\Delta t \in (0, 2)$ , then there are two points in the  $(j_{1r}, \gamma)$ -plane, denoted  $P_1$  and  $P_2$ , associated with  $Q_{2n+1}$ . (See part (1) of Lemma 6.) Specifically, let  $P_1$  be the point that is associated with the unique solution of (25-26) on  $I_\nu^- = (2n\pi, (2n+1)\pi)$  (or, equivalently, on  $I_\nu^+ = ((2n+1)\pi, (2n+2)\pi)$ ), and let  $P_2$  be the point that lies at the intersection of the lines  $j_{1r} = -\gamma$  and  $j_{1r} = f(Q_{2n+1}) + \gamma$ . Since  $j_{1i}(Q)\Delta t$  varies continuously with  $Q$ , then for values of  $Q$  in a neighborhood of  $Q_{2n+1}$  we expect the interval  $I_\nu$  of  $\nu_1$ -values associated with the mapping (25-26) to be as described in Lemma 5. For example, if  $\frac{dj_{1i}}{dQ}(Q_{2n+1}) > 0$ , then  $j_{1i}(Q)\Delta t$  increases through  $(2n+1)\pi$  as  $Q$  increases through  $Q_{2n+1}$  and the relevant interval of  $\nu_1$ -values switches from  $(2n\pi, j_{1i}(Q)\Delta t)$  to  $(j_{1i}(Q)\Delta t, 2(n+1)\pi)$  as  $Q$  increases through  $Q_{2n+1}$ . In any case, for  $Q$  sufficiently close to  $Q_{2n+1}$  so that  $f(Q)\Delta t$  remains smaller than  $w_{\max}(Q)$ , there are two solutions  $\nu_1$  of (25-26) on the appropriate  $I_\nu$ -interval. These values of  $\nu_1$  determine a pair of points on the critical curve in the  $(j_{1r}, \gamma)$ -plane via the parametric equations (23-24). We now show that these points converge to  $P_1$  and  $P_2$  as  $Q \rightarrow Q_{2n+1}$ . Specifically, one of the pair of solutions is associated with a  $\nu_1$ -value in the interval  $(2n\pi, \nu^*) \subset I_\nu^-$  if  $j_{1i}(Q)\Delta t < (2n+1)\pi$ , and with the interval  $(\nu^*, (2n+2)\pi) \subset I_\nu^+$  if  $j_{1i}(Q)\Delta t > (2n+1)\pi$ , where  $\nu^*$  determines  $w_{\max}$  via (39). (This is the  $\nu_1$  solution that is furthest from  $(2n+1)\pi$ .) This  $\nu_1$ -value determines a point in the  $(j_{1r}, \gamma)$ -plane that

converges to  $P_1$  as  $Q \rightarrow Q_{2n+1}$  since  $w(\nu_1, Q)$  changes continuously on that subinterval as  $Q \rightarrow Q_{2n+1}$ . To see that the second of the pair of  $\nu_1$  solutions describes a point that converges to  $P_2$  as  $Q \rightarrow Q_{2n+1}$ , we first note that the  $\nu_1$  value must lie between  $\nu^*$  and  $(2n+1)\pi$  and that  $\nu^* \rightarrow (2n+1)\pi$  as  $Q \rightarrow Q_{2n+1}$ . Hence this solution  $\nu_1 \rightarrow (2n+1)\pi$  as  $Q \rightarrow Q_{2n+1}$ , and the associated point in the  $(j_{1r}, \gamma)$ -plane must approach the line  $j_{1r} = -\gamma$  as  $Q \rightarrow Q_{2n+1}$  since  $j_{1r} = \gamma \cos(\nu_1)$ . Moreover, the value of  $j_{1r} \equiv f(Q) + \gamma$  converges to  $f(Q_{2n+1}) + \gamma$  as  $Q \rightarrow Q_{2n+1}$ ; it then follows that this point converges to  $P_2$ . Thus we have shown that this critical curve in the  $(j_{1r}, \gamma)$ -plane, parameterized by  $Q$ , is continuous at any points  $Q = Q_{2n+1}$  associated with the parameterization.  $\square$

The following lemma provides a sufficient condition for a nondegenerate critical curve to lie inside of the existence boundary for fixed values of  $b_1$ ,  $b_3$ ,  $K$ , and  $\rho$ , *i.e.* as in Fig. 6(b). Thus, it determines a sufficient condition for stabilization via time-delay feedback to fail.

**Lemma 8.** *Assume that there is a  $Q$ -interval  $I_Q = [\hat{Q}_1, \hat{Q}_2]$  on which  $j_{1i}(Q)\Delta t \neq 2n\pi$  for any  $n \in \mathbb{Z}$  and on which  $f(Q) \geq 0$  with  $f(Q) = 0$  only at the endpoints  $\hat{Q}_1$  and  $\hat{Q}_2$ . If there exists a value  $Q \in I_Q$  for which  $D(Q) = 0$ , where  $D(Q)$  is given by (41), then the traveling wave cannot be (linearly) stabilized for any value of the time delay feedback parameter  $\gamma$ .*

*Proof.* Assume that the conditions of the lemma are met and let  $Q^*$  be the largest value of  $Q \in I_Q$  for which  $D(Q) = 0$ . That the traveling wave cannot be stabilized for  $\gamma \geq 0$  follows from part (b) of Lemma 2. For  $\gamma < 0$  we show below that there is a continuous critical curve, parameterized by  $Q \in [Q^*, \hat{Q}_2]$ , that extends from  $\gamma = j_{1r} = 0$  to  $\gamma \rightarrow -\infty$  along the asymptote  $j_{1r} = \gamma$ .

To see that there is a continuous critical curve parameterized by  $Q \in [Q^*, \hat{Q}_2]$ , we must consider the mapping (25-26) between  $\nu_1$  and  $Q$  over this range of  $Q$ -values. Since  $D(Q)$  is continuous, with  $D(Q) = 0$  only at the endpoint  $Q = Q^*$ , then the sign of  $D(Q)$  for  $Q \in (Q^*, \hat{Q}_2]$  is the same as the sign of  $D(\hat{Q}_2)$ . Since  $w_{\max}(Q)$ , defined by (39), is positive whenever  $j_{1i}(Q)\Delta t \neq 2n\pi$ , and since  $f(\hat{Q}_2) = 0$ , we know that  $D(\hat{Q}_2) < 0$ . While for  $Q = Q^*$  there is a unique value  $\nu_1 = \nu^*$  associated with the mapping (25-26), which is given by (39), there are two corresponding values of  $\nu_1$  for all other values of  $Q$  in the interval since  $D(Q) < 0$  (*i.e.* for  $Q \in (Q^*, \hat{Q}_2)$ ). (If ever  $j_{1i}(Q)\Delta t = (2n+1)\pi$ , then one of these  $\nu_1$  values is  $(2n+1)\pi$ .) All of the values of  $\nu_1$  lie in a  $\nu$ -interval  $J_\nu = (2n\pi, 2(n+1)\pi)$  for some  $n$  since  $j_{1i}(Q)\Delta t \neq 2m\pi$  for any  $m \in \mathbb{Z}$  and any  $Q \in [\hat{Q}_1, \hat{Q}_2]$ . We may now define two functions  $\nu_1^a(Q)$  and  $\nu_1^b(Q)$  using the mapping on  $[Q^*, \hat{Q}_2]$ . We choose  $\nu_1^a(Q)$  to be the solution of (25-26) that is furthest from the midpoint of  $J_\nu$  (*i.e.* furthest from  $\nu_1 = (2n+1)\pi$ ) and  $\nu_1^b(Q)$  to be the solution that is closest to  $\nu_1 = (2n+1)\pi$ . We note that the function  $\nu_1^a(Q)$  is discontinuous at any  $Q$  where  $j_{1i}(Q)\Delta t$  goes through  $(2n+1)\pi$  due to the jumps in the interval  $I_\nu$  from  $I_\nu^+$  to  $I_\nu^-$ . (In particular, the discontinuity corresponds to  $\nu_1^a$  being reflected to  $2(2n+1)\pi - \nu_1^a$ ; see Lemma 6.) In contrast, there are no discontinuities in  $\nu_1^b(Q)$ ; it

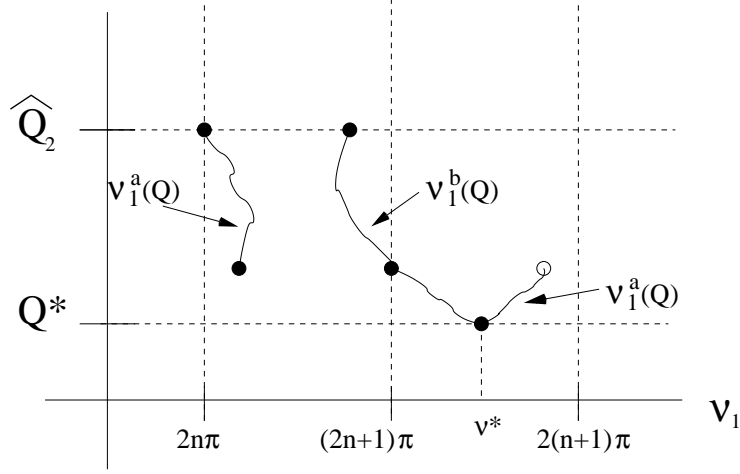


**Figure 8.** Schematic of the mappings between  $\nu_1$  and  $Q$  that parameterize a critical curve in the  $(j_{1r}, \gamma)$ -parameter plane. The parameterization by  $Q \in [Q^*, \hat{Q}_2]$  is determined by the two functions  $\nu_1^a(Q)$  and  $\nu_1^b(Q)$ , defined in the proof of Lemma 8, where  $\nu_1 \in [2n\pi, 2(n+1)\pi]$ . The schematic is typical of the degenerate case where  $j_{1i}(Q)\Delta t = (2n+1)\pi$  for some  $Q \in (Q^*, \hat{Q}_2)$ , in which case  $\nu_1^a$  is discontinuous as shown.

takes on the value  $(2n+1)\pi$  at any  $Q$  value where  $j_{1i}(Q)\Delta t = (2n+1)\pi$ . See Fig. 8 for an example of functions  $\nu_1^a(Q)$  and  $\nu_1^b(Q)$  in the discontinuous case. Note that the two functions approach the unique value  $\nu_1 = \nu^*$  as  $Q \rightarrow Q^*$ .

A  $Q$ -parameterized critical curve is obtained by inserting the pairs  $(Q, \nu_1^a(Q))$  and  $(Q, \nu_1^b(Q))$  into the parametric equations for  $j_{1r}$  and  $\gamma$  given by (23)-(24). The continuity of the critical curve associated with  $\nu_1^b(Q)$  follows directly from the continuity of the mapping in this case. The function  $\nu_1^a(Q)$  may be a discontinuous function at isolated points  $Q$  where  $j_{1i}(Q)\Delta t = (2n+1)\pi$ , as described above. However, by Lemma 7, these points do not lead to corresponding discontinuities in the critical curve. Thus the portion of the critical curve parameterized by  $(Q, \nu_1^a(Q))$  is also continuous. The two functions together parameterize a continuous critical curve from the origin in the  $(j_{1r}, \gamma)$ -plane to  $\gamma \rightarrow -\infty$  along  $\gamma = j_{1r}$ . This follows since the two curves meet as  $Q \rightarrow Q^*$ , and since  $(\hat{Q}_2, \nu_1^b(\hat{Q}_2)) = (\hat{Q}_2, j_{1i}(\hat{Q}_2)\Delta t)$  and  $(\hat{Q}_2, \nu_1^a(\hat{Q}_2)) = (\hat{Q}_2, 2\pi m)$ , where  $m = n$  or  $m = (n+1)$ . Thus the curve parameterized by  $(Q, \nu_1^b(Q))$  approaches the origin of the  $(j_{1r}, \gamma)$ -plane as  $Q \rightarrow \hat{Q}_2$  and the curve parameterized by  $(Q, \nu_1^a(Q))$  approaches, as  $Q \rightarrow \hat{Q}_2$ , the asymptote  $\gamma = j_{1r}$  with  $\gamma \rightarrow -\infty$ .  $\square$

We now use the results of the previous lemmas to prove our main stability result stated in Theorem 1.

*Proof. of Theorem 1.* The necessary condition for linear stability of the traveling wave follows from Lemma 8 in the case that  $j_{1i}(Q)\Delta t \neq 2\pi n$  for any  $n \in \mathbb{Z}$  and for any  $Q$  for which  $f(Q) \geq 0$ . Note, in particular, that the equations (34-35) in Theorem 1 are

equivalent to the condition  $D(Q) = 0$  in Lemma 8, through the definition of  $w_{max}(Q)$  given by (39).

If  $j_{1i}(Q)\Delta t = 2\pi n$  for some  $Q = Q_{2n}$  where  $f(Q_{2n}) \geq 0$ , then Lemma 4 states that the traveling wave cannot be made linearly stable (with the prescribed value of  $\rho$ ) for any value of  $\gamma$  associated with the time-delay feedback. We now need to show that in this case (34-35) has a solution. If  $f(Q_{2n}) = 0$ , then  $(Q, \nu_1) = (Q_{2n}, 2\pi n)$  solves (34-35). If  $f(Q_{2n}) > 0$ , then we can show there must be a solution to  $D(Q) = 0$  on the interval  $(Q_{2n}, \hat{Q}_2)$ , where  $\hat{Q}_2$  is the zero of  $f(Q)$  that is closest to  $Q_{2n}$ , i.e.  $f(\hat{Q}_2) = 0$  and  $f(Q) > 0$  for all  $Q \in (Q_{2n}, \hat{Q}_2)$ . (Recall that the equation  $D(Q) = 0$ , where  $D(Q)$  is defined by (41), is equivalent to (34-35).) To see that there is a  $Q \in (Q_{2n}, \hat{Q}_2)$  for which  $D(Q) = 0$ , note that  $D(Q_{2n}) > 0$  since  $w_{max}(Q_{2n}) = 0$  and  $D(\hat{Q}_2) < 0$  since  $f(\hat{Q}_2) = 0$ . The result follows from the continuity of  $D(Q)$ .

To complete the proof we show that the traveling wave may be stabilized at  $\gamma = -\frac{1}{\Delta t}$  if there is no solution of (34-35). This follows since the equations (34-35) describe points on a critical curve within the accessible region for  $\gamma = -\frac{1}{\Delta t}$ . Thus there is no critical curve that passes through  $\gamma = -\frac{1}{\Delta t}$  if there is no solution to (34-35). In this case, the stability boundary must cross the existence line as in Fig. 6(a), and the traveling wave can be stabilized for some range of  $\gamma$  values, including  $\gamma = -\frac{1}{\Delta t}$ .  $\square$

The significance of Theorem 1 is that it determines an “optimum” value of  $\gamma$  to use in stabilizing the traveling wave; this is the value  $\gamma = -\frac{1}{\Delta t}$ . To be more precise, any set of  $\gamma$  values that stabilize the traveling wave must include  $\gamma = -\frac{1}{\Delta t}$ . We note that this  $\gamma$ -value coincides with where the stability boundary is furthest from the asymptote  $j_{1r} = \gamma$  for each *fixed* value of  $j_{1i}\Delta t \neq 2n\pi$  (see part (1) of Lemma 1). The power of Theorem 1 is that it replaces the “brute force” approach of determining whether there are any growing solutions of the linear delay equation (19) for each and every value of  $Q$  for which  $f(Q) > 0$  with the simpler problem of determining whether there is a solution to an algebraic equation for  $Q$  over the same interval for which  $f(Q) > 0$ .

#### 4. Numerical Linear Stability Results

Figure 9 presents numerical linear stability results in the  $(|K|, \rho)$ -parameter plane for various values of  $(b_1, b_3)$  in the Benjamin-Feir unstable regime. These diagrams were created using the stability criterion of Theorem 1. Specifically, the criterion was applied at points on a grid in the  $(K, \rho)$ -plane with spacing of 0.0025 in the  $K$ -direction and 0.001 in the  $\rho$ -direction. In order to determine whether there is a solution to (34-35) of Theorem 1, we first eliminated the variable  $\nu$  from (34-35) yielding a single equation for  $Q$ . Care was taken with the trigonometric terms in  $\nu$ , which needed to be inverted so that the  $\nu$  values were in the interval  $I_\nu$  that contained  $j_{1i}(Q)\Delta t$  for each value of  $Q$ . (See Lemmas 5-6 for a description of  $I_\nu$ .) Newton’s method was then used to determine whether there was a solution for any  $Q$  satisfying  $0 \leq f(Q)\Delta t \leq 2$ . Specifically, for each traveling wave tested, the program first checked all values of  $Q$

between .002 and 20 at an increment of .002, determining the ranges of  $Q$  values for which  $f(Q) > 0$ . (Although we did not prove in all cases that there cannot be an instability for  $Q > 20$ , this represents an extremely conservative estimate of the largest  $Q$  value for an instability for the  $(b_1, b_3, K)$  values considered; instabilities were generally bounded well below  $Q = 20$  for the parameters used in the plots.) Next, on each interval for which  $f(Q)\Delta t \in [0, 2]$ , up to twenty-four  $Q$  values were chosen as initial conditions for Newton's method, which was used to determine whether there was a solution to the stability criterion equations (34-35) or not.

Note that the black region in Figure 9(g) indicates parameter values for which  $f(Q) < 0$  for all  $Q$  tested (*i.e.* for  $Q \in (0, 20)$  at intervals of .002). Thus, by Lemma 2, the traveling wave can be stabilized by spatially-translated feedback alone in this region. The lighter shaded regions of Figure 9 indicate parameter values for which the traveling wave could be stabilized by a combination of spatial and temporal feedback, at least for the "optimal choice" of temporal feedback parameter  $\gamma = -\frac{1}{\Delta t}$ . The feedback failed to linearly stabilize the traveling wave at all other points in the parameter plane.

Figure 9(h) summarizes our linear stability results in the  $(b_1, b_3)$ -parameter plane; it indicates both parameters for which we found stable regions in the  $(K, \rho)$ -plane (*cf.* Figure 9(a)-(g)), and parameter values, marked by triangles, where either no stable traveling waves were found or only very narrow stability regions near the unphysical limit in which  $\Delta t \rightarrow \infty$ . From Figure 9 it is evident that the stable regions in the  $(K, \rho)$ -parameter plane are more substantial close to the Benjamin-Feir line. Moreover, from a comparison of Figure 9(h) with Figure 1, we see that the feedback technique seems to be more effective in stabilizing traveling waves in the phase turbulent regime, although it also works for some parameters in the amplitude turbulent regime.

We have performed numerous "brute force" checks of the stability results summarized by Figure 9 in order to have confidence in our numerical implementation of the stability criterion of Theorem 1. An example of such a check is given in Figure 10, which shows the results of our direct calculation of the growth rates of solutions of the linear delay equation (19) (for  $j = 1$ ) as a function of  $Q$  for two different points in the parameter plane associated with Figure 9(g). Figure 10(a) corresponds to a point just inside of the stability boundary, while Figure 10(b) corresponds to a nearby point that is outside of the stability boundary.

We now examine in greater detail some of the features evident in Figure 9. We first note that in each of Figures 9(b-g) the leftmost stability tongue extends to  $\rho = 0$  indicating that the associated  $K$ -values can be stabilized with temporal feedback alone. We find that the  $K$ -values associated with the left-most stability tongue in Figures 9(a)-(g) include a value  $K$  for which spatially-resonant perturbation wavenumbers  $\tilde{Q}_2 = 2K$  have associated frequencies  $j_{1i}(\tilde{Q}_2)$  that satisfy  $j_{1i}(\tilde{Q}_2)\Delta t = -\pi$ . The significance of this latter relation is that it corresponds to the degenerate situation for which the stability boundary in the  $(j_{1r}, \gamma)$ -plane extends all the way to the line  $\gamma = -j_{1r}$  for  $\gamma = -1/\Delta t$ ; see Fig. 3(a) with  $\alpha = j_{1r}$ ,  $G = \gamma$ . In particular, while perturbations with the resonant wavenumber  $Q = \tilde{Q}_2$  are not affected by the spatial feedback, their growth rates are,

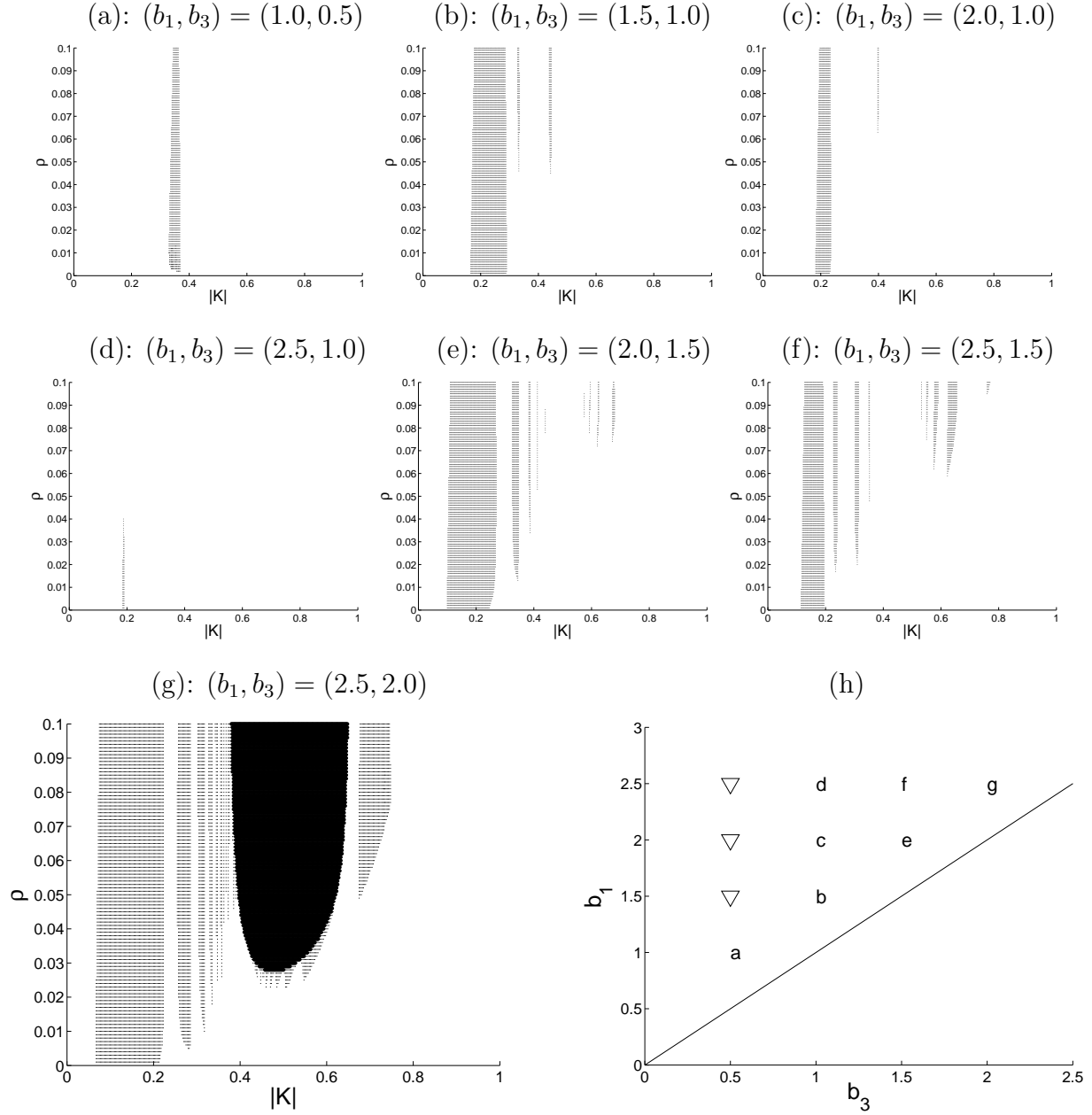


**Figure 9.** (a)-(g) Examples of stability diagrams in the  $(|K|, \rho)$ -parameter plane, created using the stability criterion of Theorem 1, for the values of  $(b_1, b_3)$  indicated above each plot. The lighter shading indicates regions that can be stabilized by a combination of spatial and temporal feedback (with  $\gamma = -1/\Delta t$ ). In the darker region in (g), the traveling wave can be stabilized by spatial feedback alone. (h) Summary of our stability results in the  $(b_3, b_1)$ -parameter plane. The letters refer to the stability diagrams shown in plots (a)-(g), which exhibit stable regions in the  $(K, \rho)$ -parameter plane. At points marked by triangles, either no stable traveling waves are found, or only very narrow stable regions near the unphysical limit in which  $\Delta t \rightarrow \infty$ .



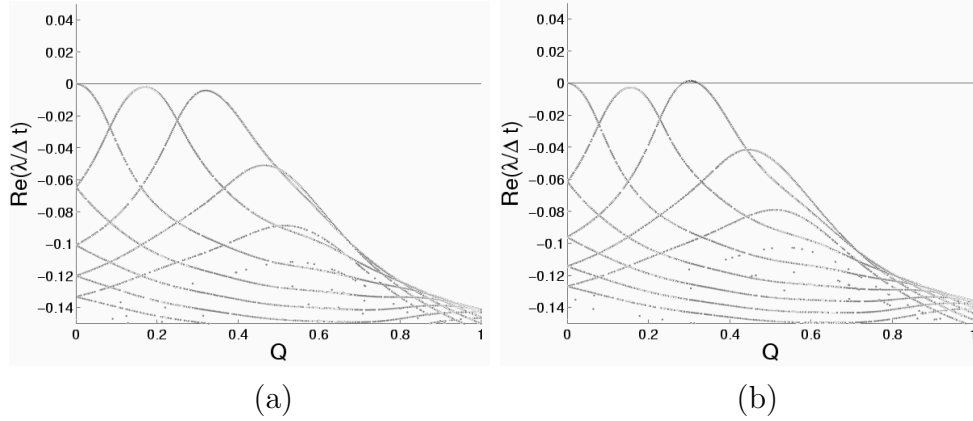
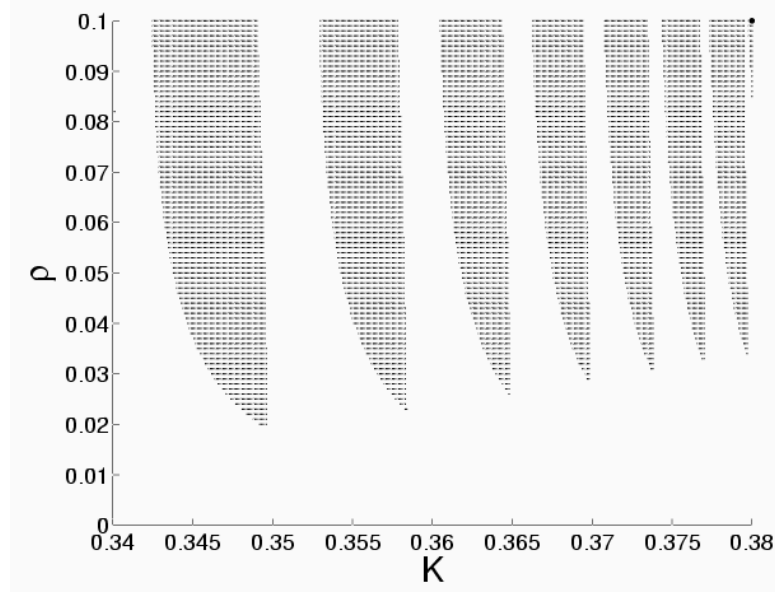


**Figure 10.** Plots of the growth rates associated with solutions of the delay equation (19) (for  $j = 1$ ) as a function of  $Q$  for  $(b_1, b_3) = (2.5, 2.0)$ ,  $\rho = .007$ , and (a)  $K = .2800$ , (b)  $K = .2875$ .

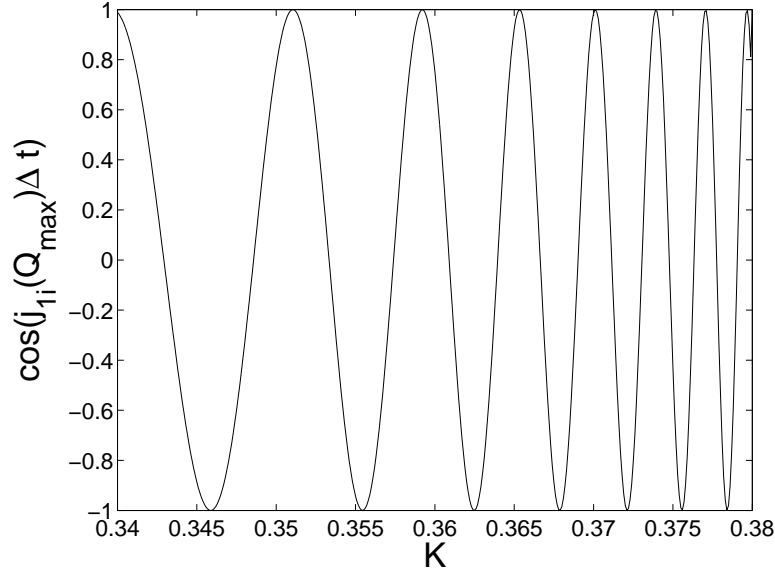
loosely speaking and in the sense just described, maximally reduced by the temporal feedback. These observations suggest a possible explanation for why this first stability tongue can extend all the way to  $\rho = 0$ , as well as for its positioning along the  $K$ -axis.

Note that the lone stability tongue of Figure 9(d) narrows as  $\rho$  increases, eventually vanishing (at our resolution in  $K$ ) once  $\rho$  exceeds 0.04. A similar, though less pronounced, narrowing of the left-most stability tongue, with increasing  $\rho$ , is present in the other stability diagrams presented in Figure 9. We conjecture that this narrowing is related to the observation above that these stability tongues are associated with values of  $K$  that are unstable in the absence of feedback to spatially resonant perturbation wavenumbers  $\tilde{Q}_n$ . To understand this claim, expand the real and imaginary parts of the eigenvalue  $j_1(Q)$  of (18) about the resonant  $Q = \tilde{Q}_n = nK$  ( $n = 2$  above), and focus on the specific contribution to  $j_1(Q)$  that is due to the spatial feedback term. Taylor expanding the diagonal factor  $\rho(e^{iQ\Delta x} - 1)$ , with  $Q = \tilde{Q}_n + \Delta Q$ , about  $\Delta Q = 0$ , we find that the effect of the spatial feedback term is to move the eigenvalue  $j_1$  in the complex plane by an amount  $\rho(i\Delta Q\Delta x - \Delta Q^2\Delta x^2/2 + \dots)$ . For large enough  $\rho$  we thus expect the width of the band of unstable wavenumbers about  $\tilde{Q}_n$  to scale as  $1/\sqrt{\rho}$  since the spatial feedback will decrease the growth rate  $f(Q)$  near  $\tilde{Q}_n$  by  $\rho\Delta Q^2\Delta x^2/2$ ; *i.e.* the larger  $\rho$  is, the smaller the unstable band about  $\tilde{Q}_n$  will be. This in turn leads to an  $\mathcal{O}(\sqrt{\rho})$  contribution to the change in  $j_{1i}$  over the same band of unstable wavenumbers since the spatial feedback shifts  $j_{1i}$  by  $\rho\Delta Q\Delta x$ . From Lemma 4 it follows that if the change in  $j_{1i}\Delta t$  over the unstable band exceeds  $2\pi$  then the traveling wave is necessarily unstable. Thus, we expect the stable regions associated with spatially resonant  $Q$  must vanish for large enough  $\rho$ .

We now focus on the accumulation of narrow stability tongues that are evident, for example, in Figures 9(e)-(g). We find that the stability tongues become narrower and narrower, shifting to larger and larger values of  $\rho$ , as  $|K| \rightarrow \frac{1}{\sqrt{1+b_1b_3}}$ , which is where the frequency  $\omega \rightarrow 0$  and consequently  $\Delta t$  diverges. Figure 11(a) shows a blowup



(a)



(b)

**Figure 11.** (a) A blow-up of a portion of the stability diagram for  $(b_1, b_3) = (2.5, 2.0)$  (cf. Fig. 9(g)). (b) Corresponding plot of  $\cos(j_{1i}(Q_{max})\Delta t)$  vs.  $K$ , where  $Q_{max}(K)$  is the perturbation wavenumber that gives the largest growth rate  $f_{max}$  for each  $K$ .

of part of Fig. 9(g). The rapid alternation between stable and unstable regions with small changes in  $K$ , occurs as  $K$  approaches the singular point where  $\omega \rightarrow 0$  and  $\Delta t \rightarrow \infty$ . We trace this rapid variation in stability to the rapid winding of the phase  $j_{1i}(Q)\Delta t$ , through successive multiples of  $2\pi$ , when  $\Delta t$  is large. This claim is explored in Figure 11(b). Specifically, for this figure the value of  $\rho$  is held fixed at  $\rho = 0.1$ , and the value of  $Q_{max}$  as a function of  $K$  is determined; here  $Q_{max}$  corresponds to the value of  $Q$  at which the growth rate  $f(Q)$  reaches its absolute maximum  $f_{max}$ . Figure 11(b)

is a plot of  $\cos(j_{1i}(Q_{max})\Delta t)$  vs.  $K$ , which shows that the spacing of the stability tongues in Figure 11(a) is the same as the spacing of the maxima of  $\cos(j_{1i}(Q_{max})\Delta t)$  in Figure 11(b). On closer examination, we find that the positions of the stability tongues in Figure 11(a) for  $\rho = 0.1$  are approximately centered around the points for which  $j_{1i}(Q_{max})\Delta t = (2n + 1)\pi$ , for successive integers  $n$ . That the locations of the stability tongues appear to coincide with the places where  $j_{1i}(Q_{max})\Delta t = (2n + 1)\pi$  is perhaps not surprising. In particular, as already noted, it is at this degenerate value that the stability boundary in the  $(j_{1i}, \gamma)$  parameter plane extends the furthest from the asymptote  $\gamma = j_{1r}$ , and for this reason it accommodates the largest value of  $f_{max}$  stably (cf. Fig. 3(a)). (See also Just *et al.* [32].) Moreover, we know that points for which  $j_{1i}(Q_{max})\Delta t = 2n\pi$  cannot be stable by Lemma 4, so it is expected that the stability tongues, if present, would avoid the even multiples of  $\pi$ . It is interesting to note that the spatial length scale for the alternation between stable and unstable regions observed in Figure 11(a) is a direct result of the introduction of time delay into the problem. When no time delay is included, the stability of the traveling wave depends only upon  $f(Q)$ , the largest growth rate associated with an eigenvalue of the stability matrix  $J$ , but once the time delay is added both the real and imaginary parts of  $j_1$  can influence stability in a complicated manner captured by our main stability result, Theorem 1.

While the presentation of our analysis focused on the case where  $\Delta x$  and  $\Delta t$  are chosen so that  $K\Delta x = |\omega|\Delta t = 2\pi$ , it is readily extended to the situation where  $\omega\Delta t = 2m\pi$  and  $K\Delta x = 2n\pi$  for nonzero integers  $m$  and  $n$ . Figure 12 presents numerical linear stability results obtained for various integers  $m, n$ . It is perhaps not surprising that the effect of increasing the delay time or the spatial shift is to reduce the extent of the stability regions in the  $(|K|, \rho)$ -plane. Afterall, the larger the value of  $\Delta t$ , the more likely it is that  $j_{1i}\Delta t$  will reach a multiple of  $2\pi$  over an unstable band of  $Q$ -values. Similarly, the larger the value of  $\Delta x$ , the more likely that  $Q\Delta x$  is a multiple of  $2\pi$  over an unstable interval of perturbation wavenumbers. However, increasing the spatial shift by the factor  $n$  does not appear to significantly affect the first stability tongue (compare Fig. 12 (a) and (b) with Fig. 9(e)). This observation is consistent with our association of this first stability tongue, which extends all the way to  $\rho = 0$  with values of  $Q$  for which  $Q\Delta x$  is a multiple of  $2\pi$ ; the stabilization achieved over that band of  $K$  is due to the temporal feedback. Increasing the time delay by the factor  $m$  has a much more significant impact on this first stability tongue (see Fig. 12(c) and (d)). It both narrows the stability tongues and appears to shift them to smaller  $|K|$ . This effect is presumably related to the overall increase, with  $\Delta t$ , in the winding of the phase  $j_{1i}(Q_{max})\Delta t$  over an interval of  $K$  values, thereby accounting for the shift in the positions of the stability tongues (cf. Fig. 11).

## 5. Conclusions

In this paper we have examined the effectiveness of the noninvasive feedback control scheme, proposed first in the setting of a nonlinear optics problem [2], for stabilizing

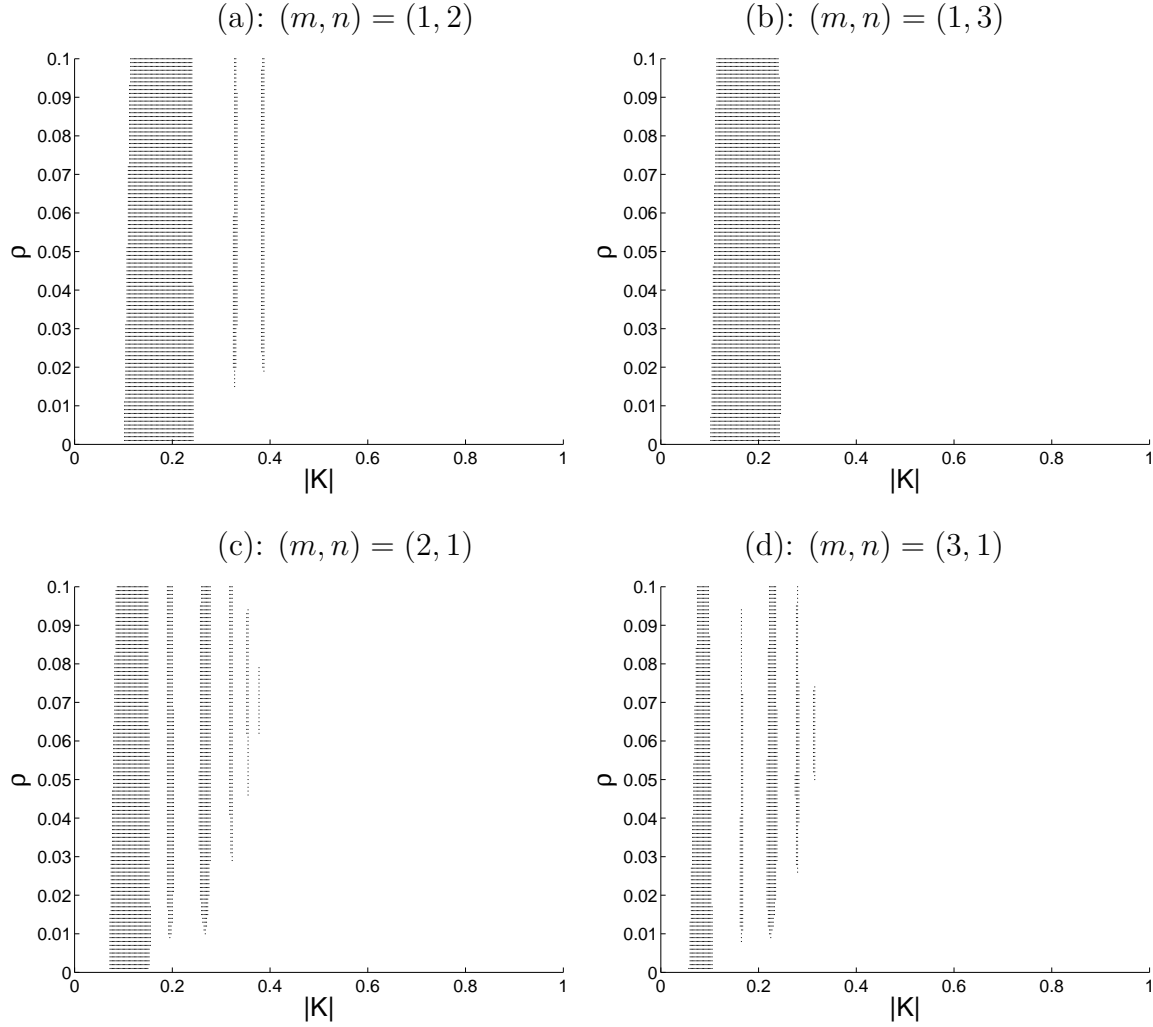


**Figure 12.** Examples of stability diagrams for  $(b_1, b_3) = (2.0, 1.5)$  and  $\omega\Delta t = 2m\pi$ ,  $K\Delta x = 2n\pi$ , where  $(m, n)$  are indicated above each figure. The stability diagram associated with the standard case  $(m, n) = (1, 1)$  is presented in Fig. 9(e).

traveling wave solutions of the one-dimensional complex Ginzburg Landau equation. Our approach is based on a linear stability analysis, which involves examining the solutions of a linear (complex) delay equation whose coefficients depend on the perturbation wavenumber  $Q$ . The traveling wave solution is stabilized by the feedback if all solutions of the  $Q$ -parameterized family of delay equations decay. Our analysis leads to a single stability criterion, Theorem 1, that allows us to determine stability of a traveling wave against perturbations of all wave numbers by determining whether a nonlinear algebraic equation for  $Q$  possesses a solution or not. Perhaps more significant is that our main stability theorem specifies a value of the feedback parameter  $\gamma$ , namely  $\gamma = -\frac{1}{\Delta t}$ , which is guaranteed to work, if stabilization is at all possible. Thus, loosely speaking, one of the “control knobs” can be set in advance, thereby minimizing the amount of control parameter space that need be scanned in trying to stabilize traveling wave solutions.

In addition to our necessary and sufficient stability criterion of Theorem 1 we determined simple sufficient conditions under which the control scheme will be ineffective and interpreted these in terms of resonance conditions. For instance, we find that if there is an unstable wavenumber  $Q$  that is an integer multiple of the wavenumber  $K$  of the targeted solution, then the spatially-translated feedback cannot eliminate this instability. Likewise if there is an unstable wavenumber and the frequency associated with that perturbation,  $j_{1i}(Q)$ , is an integer multiple of the frequency  $\omega$  of the underlying traveling wave state, then the temporal feedback is ineffective in suppressing the instability [32]. A simple consequence of these observations is that it is not possible to use the temporal feedback to stabilize the spatially uniform oscillatory pattern at  $K = 0$ ; this follows quite generally from the fact that the Benjamin-Feir instability is a longwave instability of a translation invariant problem. Specifically, translation symmetry forces a neutral mode to exist at  $Q = 0$  and the longwave nature of the instability ensures that there are instabilities in a neighborhood of  $Q = 0$ . For  $K = 0$ , and  $Q$  sufficiently small, these instabilities are associated with purely real eigenvalues of the linear stability matrix  $J$ . Such steady modes of instability cannot be suppressed by spatially-translated feedback if  $K = 0$ , and they cannot be eliminated by the temporal feedback either since  $j_{1i}(Q) = 0$  if the eigenvalues are purely real. This observation is interesting in light of similar results obtained by Harrington and Socolar [18]; building on results in [33, 34] they show that the extended time-delay autosynchronization approach to controlling traveling waves of the CGLE in one-dimension [17] necessarily fails in two-dimensions due to symmetries that force the Floquet multipliers to be purely real.

For various values of  $(b_1, b_3)$  in the Benjamin-Feir unstable regime, we have used our stability criterion to determine numerically where in the  $(|K|, \rho)$ -parameter plane the feedback control scheme is effective in stabilizing traveling wave solutions with wavenumber  $K$ . We find that the stability regions take the form of stability tongues, and we offer some insights into the position and spacing with  $|K|$  of these stable regions, as well as their extent in the feedback parameter  $\rho$ . While we find some limited regions where temporal feedback alone works ( $\rho = 0$ ) and another case where spatial feedback alone works ( $\gamma = 0$ ), most stable regions require a combination of spatial and temporal feedback to stabilize the traveling wave. However, a notable feature of the stability diagrams in Figure 9, is that the minimal  $\rho$  required to stabilize the waves is often quite small.

We expect Theorem 1 will have applications beyond the example considered here of feedback control within the setting of the complex Ginzburg Landau equation. In particular, we expect our analysis to apply to other linear stability problems that lead to a parameterized family of delay equations of the form (19), provided that the growth rates  $j_{kr}(Q)$ , in the absence of temporal feedback, have an absolute maximum as a function of  $Q$ . Our analysis of the CGLE with feedback was further simplified by the fact that we could eliminate one of the delay equations from consideration altogether. We did not, however, consider the case where the feedback parameters  $\gamma$  and  $\rho$  are allowed to be complex.

This paper suggests a number of directions for further investigation. For example, it would be interesting to carry out numerical investigations to determine the evolution of the system in the parameter regimes where the traveling waves are not stabilized, *i.e.* choose  $\Delta x$  and  $\Delta t$  appropriate for a traveling wave of wavenumber  $K$  that is not stabilized by the feedback. Would the system then evolve to a different traveling wave state, one for which the feedback does not vanish? More generally, numerical investigations, guided by our analysis, could help assess how well the feedback works when stabilization is possible, but when it is not possible to prepare the system in a neighborhood of the targeted traveling wave pattern. For instance, will the feedback work when it is “turned on” after a spatio-temporal chaotic state has developed? Another avenue for numerical investigation stems from a potential drawback associated with the feedback scheme investigated here – it assumes that the traveling wave dispersion relation  $\omega(K)$  is known. Hence it would be worthwhile to investigate numerically the consequences of a “mismatch” between the spatial shift  $\Delta x$  and the temporal delay  $\Delta t$ . This might be particularly interesting in the case of the two-dimensional CGLE, in which case the traveling wave pattern can “rotate” in order to compensate for any mismatch.

Another direction for future research is suggested by our choice of the CGLE for the detailed analysis presented here. Specifically we refer to the fact that the CGLE arises as the universal amplitude equation describing the *long* spatial and *slow* temporal evolution of homogeneous oscillations in spatially extended isotropic systems. Are these the appropriate scales on which to be applying the feedback? If so, how should the feedback parameters for the “original problem” be chosen to achieve the optimal value of  $\gamma = -1/\Delta t$  that we find for the “reduced model” given by the CGLE? As a first step in addressing these questions it would be worthwhile to carry out an analysis, similar to the one we have done here, but on the original equations describing the physical system undergoing a Hopf bifurcation, *e.g.* on a model of chemical reaction–diffusion system in the oscillatory regime.

An attractive feature of the feedback control scheme investigated here is its noninvasive nature, *i.e.* the feedback vanishes when the targeted state is reached. This design feature exploits the underlying spatial and spatio-temporal symmetry properties of the desired pattern in a very natural way, suggesting that this feedback approach may be readily generalized to more complicated patterns. For instance, the original problem investigated by Lu, Yu, and Harrison [2] involved oscillatory stripe patterns in a *two-dimensional* isotropic system. They found that they could target a particular orientation of the stabilized stripe pattern by an appropriate rotation of the spatial translation applied in the feedback control. Thus it would be of interest both to extend our linear stability analysis to the control of traveling plane wave solutions of the *two-dimensional* CGLE, and to consider the feedback stabilization of more complicated traveling wave patterns.

## Acknowledgments

We thank Sue Ann Campbell and Josh Socolar for helpful discussions regarding this work. The research of MS was supported by NSF grant DMS-9972059 and by the NSF MRSEC Program under DMR-0213745. KAM received support through an NSF-IGERT fellowship under NSF grant DGE-9987577.

## References

- [1] K. Pyragas. Continuous control of chaos by self-controlling feedback. *Physics Letters A*, 170:421, 1992.
- [2] W. Lu, D. Yu, and R. G. Harrison. Control of patterns in spatiotemporal chaos in optics. *Phys. Rev. Lett.*, 76:3316, 1996.
- [3] M Golubitsky, I Stewart, and D.G. Shaeffer. *Singularities and Groups in Bifurcation Theory, Volume II*. Springer-Verlag, New York, 1988.
- [4] B. I. Shraiman, A. Pumir, W. van Saarloos, P. C. Hohenberg, H. Chaté, and M. Holen. Spatiotemporal chaos in the one-dimensional complex Ginzburg-Landau equation. *Physica D*, 57:241, 1992.
- [5] E. Ott, C. Grebogi, and J. A. Yorke. Controlling chaos. *Phys. Rev. Lett.*, 64:1196, 1990.
- [6] K. Pyragas and A. Tamaševičius. Experimental control of chaos by delayed self-controlling feedback. *Physics Letters A*, 180:99, 1993.
- [7] D. J. Gauthier, D. W. Sukow, H. M. Concannon, and J. E. S. Socolar. Stabilizing unstable periodic orbits in a fast diode resonator using continuous time-delay autosynchronization. *Phys. Rev. E*, 50:2343, 1994.
- [8] S. Bielawski, D. Derozier, and P. Glorieux. Controlling unstable periodic orbits by a delayed continuous feedback. *Phys. Rev. E*, 49:R971, 1994.
- [9] Th. Pierre, G. Bonhomme, and A. Atipo. Controlling the chaotic regime of nonlinear ionization waves using the time-delay autosynchronization method. *Phys. Rev. Lett.*, 76:2290, 1996.
- [10] Th. Mausbach, Th. Klinger, A. Piel, A. Atipo, Th. Pierre, and G. Bonhomme. Continuous control of ionization wave chaos by spatially derived feedback signals. *Physics Letters A*, 228:373, 1997.
- [11] T. Fukuyama, H. Shirahama, and Y. Kawai. Dynamical control of the chaotic state of the current-driven ion acoustic instability in a laboratory plasma using delayed feedback. *Physics of Plasmas*, 9:4525, 2002.
- [12] F. W. Schneider, R. Blittersdorf, A. Förster, T. Hauck, D. Lebender, and J. Müller. Continuous control of chemical chaos by time delayed feedback. *J. Phys. Chem.*, 97:12244, 1993.
- [13] A. Lekebusch, A. Förster, and F. W. Schneider. Chaos control in an enzymatic reaction. *J. Phys. Chem.*, 99:681, 1995.
- [14] P. Parmananda, R. Madrigal, M. Rivera, L. Nyikos, I. Z. Kiss, and V. Gáspár. Stabilization of unstable steady states and periodic orbits in an electrochemical system using delayed-feedback control. *Phys. Rev. E*, 59:5266, 1999.
- [15] A. Labate, M. Ciofini, and R. Meucci. Controlling quasiperiodicity in a CO<sub>2</sub> laser with delayed feedback. *Phys. Rev. E*, 57:5230, 1998.
- [16] J.E.S. Socolar, D.W. Sukow, and D.J. Gauthier. Stabilizing unstable periodic orbits in fast dynamical systems. *Phys. Rev. E*, 50:3245, 1994.
- [17] M. E. Bleich and J. E. S. Socolar. Controlling spatiotemporal dynamics with time-delay feedback. *Phys. Rev. E*, 54:R17, 1996.
- [18] I. Harrington and J.E.S. Socolar. Limitations on stabilizing plane waves via time-delay feedback. *Phys. Rev. E*, 64:056206, 2001.
- [19] M. E. Bleich, D. Hochheiser, J. V. Moloney, and J. E. S. Socolar. Controlling extended systems with spatially filtered, time-delayed feedback. *Phys. Rev. E*, 55:2119, 1997.

- [20] N. Baba, A. Amann, E. Schöll, and W. Just. Giant improvement of time-delayed feedback control by spatio-temporal filtering. *Phys. Rev. Lett.*, 89:074101, 2002.
- [21] E. V. Degtiarev and M. A. Vorontsov. Dodecagonal patterns in a Kerr-slice/feedback-mirror type optical system. *Journal of Modern Optics*, 43:93, 1996.
- [22] R. Martin, A. J. Scroggie, G.-L. Oppo, and W. J. Firth. Stabilization, selection, and tracking of unstable patterns by Fourier space techniques. *Phys. Rev. Lett.*, 77:4007, 1996.
- [23] A. V. Mamaev and M. Saffman. Selection of unstable patterns and control of optical turbulence by Fourier plane filtering. *Phys. Rev. Lett.*, 80:3499, 1998.
- [24] M. A. Vorontsov and B. A. Samson. Nonlinear dynamics in an optical system with controlled two-dimensional feedback: Black-eye patterns and related phenomenon. *Phys. Rev. A*, 57:3040, 1998.
- [25] E. Benkler, M. Kreuzer, R. Neubecker, and T. Tshudi. Experimental control of unstable patterns and elimination of spatiotemporal disorder in nonlinear optics. *Phys. Rev. Lett.*, 84:879, 2000.
- [26] G. Franceschini, S. Bose, and E. Schöll. Control of chaotic spatiotemporal spiking by time-delay autosynchronization. *Phys. Rev. E*, 60:5426, 1999.
- [27] M. Kim, M. Bertram, M. Pollmann, A. von Oertzen, A.S. Mikhailov, H.H. Rotermund, and G. Ertl. Controlling chemical turbulence by global delayed feedback: Pattern formation in catalytic CO oxidation on Pt(110). *Science*, 292:1357, 2001.
- [28] M. Bertram and A.S. Mikhailov. Pattern formation in a surface chemical reaction with global delayed feedback. *Phys. Rev. E*, 63:066102, 2001.
- [29] C. Beta, M. Bertram, A.S. Mikhailov, H.H. Rotermund, and G. Ertl. Controlling turbulence in a surface chemical reaction by time-delay autosynchronization. *Phys. Rev. E*, 67:046224, 2003.
- [30] D. Battogtokh and A. Mikhailov. Controlling turbulence in the complex Ginzburg-Landau equation. *Physica D*, 90:84, 1996.
- [31] D. Battogtokh, A. Preusser, and A. Mikhailov. Controlling turbulence in the complex Ginzburg-Landau equation II. two-dimensional systems. *Physica D*, 106:327, 1997.
- [32] W. Just, T. Bernard, M. Ostheimer, E. Reibold, and H. Benner. Mechanism of time-delayed feedback control. *Phys. Rev. Lett.*, 78:203, 1997.
- [33] H. Nakajima. On analytical properties of delayed feedback control of chaos. *Phys. Lett. A*, 232:207, 1997.
- [34] H. Nakajima and Y. Ueda. Limitation of generalized delayed feedback control. *Physica D*, 111:143, 1998.
- [35] K. Pyragas. Control of chaos via an unstable delayed feedback controller. *Phys. Rev. Lett.*, 86:2265, 2001.
- [36] W. Just, E. Reibold, K. Kacperski, P. Fronczak, J. A. Holyst, and H. Benner. Influence of stable Floquet exponents on time-delayed feedback control. *Phys. Rev. E*, 61:5045, 2000.
- [37] W. Just, H. Benner, and E. Reibold. Theoretical and experimental aspects of chaos control by time-delayed feedback. *Chaos*, 13:259, 2003.
- [38] K. Pyragas. Analytical properties and optimization of time-delayed feedback control. *Phys. Rev. E*, 66:026207, 2002.
- [39] M. E. Bleich and J. E. S. Socolar. Stability of periodic orbits controlled by time-delay feedback. *Physics Letters A*, 210:87, 1996.
- [40] D. V. Ramana Reddy, A. Sen, and G. L. Johnston. Dynamics of a limit cycle oscillator under time delayed linear and nonlinear feedbacks. *Physica D*, 144:355, 2000.
- [41] T.B. Benjamin and J.E. Feir. The disintegration of wave trains on deep water Part 1. Theory. *J. Fluid Mech.*, 27:417, 1967.
- [42] J.T. Stuart and R.C. DiPrima. The Eckhaus and Benjamin-Feir resonance mechanisms. *Proc. R. Soc. Lond. A*, 362:27, 1978.
- [43] B. Janiaud, A. Pumir, D. Bensimon, V. Croquette, H. Richter, and L. Kramer. The Eckhaus instability for traveling waves. *Physica D*, 55:269, 1992.
- [44] H. Chaté. Spatiotemporal intermittency regimes of the one-dimensional complex Ginzburg-Landau



- equation. *Nonlinearity*, 7:185, 1994.
- [45] O. Diekmann, S. A. van Gils, S. M. Verduyn-Lunel, and H. O. Walther. *Delay Equations, Functional, Complex, and Nonlinear Analysis*. Springer, New York, 1995.
- [46] R. D. Driver. *Ordinary and Delay Differential Equations*. Springer-Verlag, New York, 1997.